national accelerator laboratory FERMILAB-Conf-74/74-THY/EXP
July 1974

A Review of Some Recent Experimental Results from Fermilab

MARTIN B. EINHORN
Fermi National Accelerator Laboratory, Batavia, Illinois 60510

ABSTRACT

A review of some recently available (mostly preliminary) data from Fermilab is presented. Four general areas are covered: (1) particle searches, (2) deep inelastic muon scattering, (3) inelastic diffraction scattering, and (4) the production of hadrons, muons, and electrons at large transverse momenta. The purpose is to give some overview of what has been and is being done in these areas, so I give progress reports on relevant experiments which do not yet have data to present.

Operated by Universities Research Association Inc. Under Contract with the United States Atomic Energy Commission

Following the general tour* of the laboratory's physical and experimental facilities, I will turn to a description of some recent experimental results. For my purposes, it is a pity that this meeting is not two weeks after the London Conference rather than before, for much more data would be available for comparison and extension of results. As it is, most of the data that I will show you has come into my hands within the past month, and I doubt that I have fully digested its implications. Although what I will show you is only a small portion of what will be presented in London, in the time allotted me, I will only be able to highlight these results. Much of the data is preliminary, and I look forward to this review rapidly becoming obsolete as firmer results come forth. (At least the preceding lecture may survive more than two weeks!)

Of the data available to me, I have chosen to speak about that which is of widespread interest and which, in my opinion, will have long lasting implications. Because of the limitations of time, I shall not discuss results which have already been published but simply guide you to the relevant literature. One general class of experiments which I shall omit concern results from the 30" Bubble Chamber. An excellent summary has recently been concluded by Jim Whitmore.[1] The topics I have selected to discuss concern particle searches, muon

*See the preceding lecture, "An Introduction to Fermilab," also available as FERMILAB-Conf-74/73-THY/EXP, July 1974.

scattering, diffraction scattering, and the production of hadrons and muons at large momentum transfers. Because Professor Perkins has discussed the neutrino results at this meeting, there will be no mention of this most exciting class of experiments.

Let me say that, just as in my description of the accelerator characteristics, my discussion of the experiments will be brief. A great deal more information is contained in the tables and diagrams than will be explicitly provided in the body of the talk. By careful reference to figures, you can answer for yourself many of the questions which go beyond my discussion. In this way, I hope to satisfy those of you with detailed interests in specific topics without boring the rest.

Let me begin with particle searches. Until one obtains positive identification, these can be a rather lackluster and thankless class of experiments. Aside from their all-or-nothing character, a good search places significant restrictions on theoretical conjectures. I will report only that, to my knowledge, no new weird or expected or unanticipated particles have been observed at Fermilab to date. For further reference, a list of searches is given in Fig. 1.

Next, I will spend some time describing the two muon scattering experiments which are currently underway. First of all, the muon beam is constructed as shown in Fig. 2. The general characteristics of the beam lead to a yield of between 1.5 and 2.5 times 10^{-7} positive muons (at 150 GeV/c) per incident proton (at 300 GeV/c). The beam

on arrival at the muon lab is about $3\frac{1}{2}$ inches in diameter with a halo/beam ratio of 1.4. By tagging the muons, a momentum resolution of $\frac{1}{2}$% can be achieved. Conversion of the muon beam to handle 250-300 GeV muons will begin sometime next year.[2]

Muon Experiment No. 26 (Cornell-Michigan State-U.C. San Diego collaboration) is designed to directly test scaling in deep inelastic muon scattering. The kinematics of this process has been described in several theoretical lectures at this symposium, but I present Fig. 3 as a reminder of what is being tested. The kinematical range available with the current muon beam is indicated in Fig. 4. Bjorken's scaling hypothesis is the statement that, as $\nu \to \infty$ for fixed x, the structure functions W_1 and νW_2 will tend to a finite function of the dimensionless variable x. Experiment No. 26 will test this directly by measuring the counting rates on Fe at two different values of ν but at the same value of x. One way to describe how they will do this is to consider the effect of the scale transformation indicated in Fig. 3b and Fig. 5. The clever designers of Exp. No. 26 arranged it so that the experimental apparatus could be physically moved in just such a way to implement this scale transformation. Measuring first at E = 150 GeV in one configuration and later at E = 56 GeV in another, they are able to compare directly the rates at the same x in the same detectors. Many systematic problems are hopefully avoided by this technique of "scaling" the apparatus

At the Chicago American Physical Society meeting last February, Professor W. Chen presented very preliminary results based on an analysis of data taken at one energy only, 150 GeV/c. Using the structure functions determined at SLAC, treating iron as a free collection of protons and neutrons, and performing a Monte Carlo simulation of their geometries and efficiencies, the experimenters arrived at an expected rate for muons in their apparatus. Forming the ratio R of their observed rate to this expected rate, they found that it agrees with one up to about $Q^2 \approx 10$ GeV/c^2 but that it steadily decreases to about 0.7 at $Q^2 \approx 40$ (GeV/c)^2. (See Fig. 6). That is, the measured rate is lower than the expected rate for $Q^2 > 10$ (GeV/c)^2. This result is interesting but subject to all the systematic uncertainties avoided by the scaling technique described above. In addition to the Monte Carlo simulation, it depends somewhat on how much you believe the SLAC best fit to νW_2 and to what extent the determination is sensitive to the value of scalar/transverse ratio, and so forth.

The interpretation of Fig. 6 is complicated since the plot versus Q^2 is not at fixed x. Instead the mean value of x increases as Q^2 increases across the graph, although precisely how x varied, I wasn't able to find out. Secondly, the overall normalization is uncertain; where to put 1 on the ordinate is the question. Some indications of the uncertainty is illustrated by the band between the horizontal dashed lines. Thirdly, the experiment is from an iron

target rather than from hydrogen or deuterium. Although some data was taken with lead in the early stages of running, it has not been carefully analyzed. Over the SLAC range, the dependence on atomic number A was linear,[3] which, if still true at larger Q^2, would remove this uncertainty.

Since then, they have taken data at 56 GeV/c with the apparatus in the appropriately scaled configuration. This is in the process of analysis and, I'm told, it may be until the fall before any results will be available. There are, of course, some systematic changes which require careful study, e.g., the beam size is larger at 56 at 150 GeV/c and detector efficiencies don't scale. I can add the following information to that presented at the Chicago APS meeting. It appears that the "prediction" corresponds more nearly to the upper than the lower dashed line in Fig. 6. Possible asymmetries between performing the experiment with a μ^- and a μ^+ beam has been examined. For example, the interference between one and two photon exchange and radiative corrections leads to such an asymmetry. To good accuracy, no asymmetry was observed. Curves will be presented at London. There are several ways to express the result numerically. For example, there is no difference in the mean recoil energy

$$\frac{\langle E' \rangle^+ - \langle E' \rangle^-}{\langle E' \rangle^+ + \langle E' \rangle^-} = 0.00014 \pm 0.010$$

Expressed another way, there is no difference in the mean momentum transfer

$$\frac{\langle Q^2\rangle^+ - \langle Q^2\rangle^-}{\langle Q^2\rangle^+ + \langle Q^2\rangle^-} = 0.0013 \pm 0.015$$

These numbers are quite preliminary, the error purely statistical, and the result of analysis of only 20% of the data. This removes one possible question mark about the interpretation of the measurements. I understand further that, over the SLAC range of ν and Q^2, the results of Exp. No. 26 agree well with the SLAC results. Although the definitive test will be a direct comparison of the 56 GeV/c data with the 150 GeV/c data, the remarks above suggest we can have confidence in the implications of Fig. 6.

Theoretical remarks vary from "It's a pity scaling broke down" to "It's remarkable that scaling holds to within 30% over such a wide energy range." I haven't time here to discuss the possible implications of the data. Several theoretical approaches suggest, however, that it is likely that the rate of approach to the asymptotic behavior will be x dependent, so it will be important to have plots like Fig. 6 for fixed x. Perhaps it would be useful if Exp. No. 26 took data at several other energies in appropriately scaled configurations. Meanwhile, we await their definitive result of the comparison of the 56 GeV run with the 150 GeV data.[4]

Let me briefly describe the second muon experiment. The purpose

Muon Experiment No. 98 (Chicago-Harvard) is to obtain detailed information about muon scattering. This experiment is an elaborate facility designed to give data about final states as well as a determination of the structure functions of the nucleon by using liquid hydrogen and deuterium targets. The set-up is indicated in Figs. 7 and 8. Forward going charged particles produced from a collision in the target are analyzed by a system of spark chambers and a huge magnet, which was originally the heart of Fermi's old cyclotron at the University of Chicago. The scattered muon is also analyzed as well as any photons and electrons which are produced by the interaction. (This, incidentally, makes possible a measurement of μe elastic scattering off of atomic electrons in the target.) Neutron showers are also formed. Obviously, this experiment will provide an enormous amount of detailed information for quite some time. Last January, the experimenters turned up and ran for much of April and May, having 300 hours of data collection with 150 GeV/c μ^+ on a liquid hydrogen target. This has led to about 30,000 useful μp inelastic events, of which perhaps 14,000 have $Q^2 > 16$ GeV/c^2. (In addition, they have collected over 50,000 elastic μe events.) All these events are being analyzed now, and the experiment is currently collecting data on 150 GeV/c μ^+ on liquid deuterium. Additional events will also be collected on LH_2, and the experiment is scheduled to continue at least until the end of July. If scaling is violated, it will be useful to increase the running time for

this experiment to obtain data at this and other energies with excellent statistics for a doubly differential Q^2, ν plot.[5]

Professor Perkins covered neutrino physics in his talk, so I shall move on to hadron physics.

A great many experiments have been performed or are underway, of which I can only touch on a few. Many results from the early exposure in the 30" hydrogen Bubble Chamber have been previously reported and are comprehensively summarized in a recent review by Whitmore.[1] Consequently, I shall omit discussion of this work here.

Quite a few experiments have been performed which bear on the nature of diffraction scattering. First of all, let me discuss Exp. No. 104 (Brookhaven-Rockefeller-Fermilab Collaboration) whose objective is a precise ($\sim 0.1\%$) determination of $\pi^{\pm}$, $K^{\pm}$, p and $\bar{p}$ total cross sections on liquid hydrogen and deuterium over a very large energy range. The experiment is of the standard absorption variety (Fig. 9), but, owing to its precision, great care must be paid to details. There are three identical duers, onto which the beam may be directed, contain LH_2, LD_2 or vacuum. These targets are carefully monitored as to temperature and length. Behind the target are counters whose purpose is to discover how many particles are removed from the beam due to strong interactions. With the target in, the rate is measured over a range of small momentum transfers t and extrapolated under the Coulomb peak by fitting

exp $(At + Bt^2 + Ct^3)$. For further discussion, I refer you to the report at the London Conference.[6] The measurements have been performed at 50, 100, 150 and 200 GeV/c. The preliminary results are as follows: In Fig. 10, we see the pp total cross section at these four energies agreeing rather nicely with Serphukov and the ISR. The 30" Bubble Chamber points are also plotted, and are in qualitative agreement with these results. The result of Exp. No. 4 appear to be a bit high at but, given the errors, not out of bounds. We also see in Fig. 9 , the $\bar{p}p$ total cross section, which is still falling but presumably bottoming out. Next (Fig. 11) we turn to the $\pi^{\pm}p$ cross sections. $\pi^{\pm}p$ is definitely rising and $\pi^{-}p$ probably is also, although if you insisted, it could be considered constant. In Fig. (12), we see the $K^{\pm}p$ results, $K^{+}p$ continues the strong increase observed at Serpukhov; $K^{-}p$ is also beginning to increase.

Turning to deuterium, we see the pd and $\bar{p}d$ cross sections in Fig. 13. In Fig. 14 , we see the $\pi^{\pm}d$ cross sections. These two should agree if isospin invariance holds. In Fig. 15 , we see the $K^{\pm}d$ cross sections, also showing an increase. Untangling the neutron cross sections from deuterium requires a theory for rescattering corrections. At a level of 0.1%, there is no theory in which we have confidence. This is a good area for theoretical effort--how to improve Glauber theory to include inelastic intermediate states.[7] Consequently, I have no neutron cross sections to show for this experiment. Cross sectional

differences are plotted in the next figure (Fig. 16). These continue nicely onto the Serphukhov points and eyeball fits show they are decreasing like $s^{-0.5}$ or so, consistent with Regge theory. Similar results for deterium are shown in Fig. 17. The primary qualitative conclusion from this data is that the rise previously observed in the exotic channels K^+p and pp is probably characteristic of the behavior of all cross sections over these and somewhat higher energies. (You will have to draw your own conclusions on the implications for the asymptotic behavior.) The overall normalization of this data may change slightly, and settling on a value for the neutron cross sections will remain a subject of discussion for some time. However, even with these reservations, one can begin to investigate SU_3 relations and quark model predictions. I have no graphs to show you, for they would only change tomorrow, but every indication is that the trends observed at Serpukhov[8] are borne out by this data and any worrisome points (e.g., $\Delta\,\sigma(\pi^{\pm}p)$) will be resolved in favor of theoretical simplicity. That is, both Regge theory and SU_3 work very well. In the future, Exp. No. 104 will measure the total cross sections from 50 to 200 GeV/c in 10 GeV/c increments, so you will need little imagination to fill in the curves. Machine and beam transport permitting, they will go to higher momenta. Later, they may also go down to 20 GeV/c to connect into measurements there. Having a high precision determination of the total cross sections in one experiment from 20 to over 200 GeV should provide quite a theoretical

challenge for some time to come.[9]

It seems appropriate to proceed to a discussion of Exp. No. 4 (Michigan)--a measurement of the neutron cross section. The layout is shown in Fig. (18). Since the neutron beam contains a wide band of energies, one needs to determine not only the beam flux and that a neutron has interacted, but also the energy of the incoming neutron. For this purpose, Exp. No. 4 follows the target with a total absorption calorimeter. By accumulating all produced and scattered particles, the incoming energy can be determined to within about 10%. Preliminary results are shown in Fig. 19, where they are compared with a similar experiment performed at Brookhaven at lower energies. In addition, "data" is shown from Serpukhov and from Experiment No. 4. These points are deduced from deuterium data using a simple Glauber theory. As remarked earlier, their absolute values are not to be taken seriously. What is striking, and probably a point of disagreement between the experiments, is the point-to-point energy dependences. Experiment No. 4 suggests a much steeper rise than Exp. No. 104. The neutrons have also been directed onto a deuterium target, with preliminary results given in Fig. 20. Here the comparison with Serpukhov and Exp. No. 104 is direct, since isospin invariance implies that pd and nd cross sections are equal. Again we see a substantial difference in the energy dependence seen in the two Fermilab experiments.

I am not in a position to judge the source of possible discrepancy,

but one naturally would favor the relative normalization from one energy to the next in the experiment using monochromatic beams than in the one using the broad bond neutron beam.

I should mention also that Exp. No. 4 has also measured the pp total cross section at 200 and 300 GeV, which results have already been published.[10] (These data were included in Fig. 10.) At 300 GeV/c the result is consistant with other measurements performed at ISR and in the Fermilab 30" Bubble Chamber. At 200 GeV/c there appears to be a discrepancy between the magnitude of the cross section reported by Exp. No. 4 and the preliminary data from Exp. No. 104.

Experiment No. 4 has also measured the neutron cross section on a variety of heavier nuclei ranging from beryllium to uranium. Early indications[11] are that it increases like a power of the atomic number A, and the power (0.76) is somewhat larger than 2/3.

A natural extension of this discussion would be to present the elastic cross sections. pp elastic has already been reported (Exp. No. 36). (Fig. 21). Others will be determined at small t ($|t| < 1$ GeV/c) by three experiments (Exp. No. 96, Exp. No. 7 and Exp. No. 69). Experiment No. 96 (10 institutions) is an impressive 200 meter, single arm spectrometer (see Fig. 22) whose resolution enables the identification of elastic events. Data has been taken for negative particles ($\bar{p}, \pi^-, K^-$) at 100 and 140 GeV/c and for positives (p, π^+, K^+) at 50, 100, and 140 GeV/c. This is under analysis but whether it would be available by the

London meeting was uncertain when I left. They also have data on single particle inclusive cross sections.[12] Experiment No. 7 (Michigan-Fermilab) measures both the scattered beam and recoil of the target. They have data on p, $\bar{p}$, $K^{\pm}$ and $\pi^{\pm}$ on hydrogen at 40, 100, and 200 GeV/c in the range from $|t| \approx 0.1$ out to about 1 $(GeV/c)^2$. This will be presented in London.[13]

A third experiment doing elastic scattering is Exp. No. 69 (Yale-Fermilab) over the momentum range up to 1 GeV/c. For $\pi^{\pm}$, $K^{\pm}$, p and $\bar{p}$, special attention will be given to very small momentum transfers, including resolution of the Coulomb interference region. In addition, they will look at hyperon (Σ^-, Ξ^-, Ω^-, Λ^0) elastic scattering. This experiment, less well-advanced than the other two, is just tuning up. Another important experiment is Exp. No. 111 (CalTech-LBL) $\pi^- p \to \pi^0 n$. This is an extremely precise measurement of the charge exchange cross section. With a resolution of $\Delta t \approx 0.001$ $(GeV/c)^2$, this experiment provides at t=0 an important test of dispersion relations (since its imaginary part is the difference $\Delta\sigma(\pi^{\pm}p)$ reported above and its real part can be obtained (modulo assumptions on asymptotic behavior) from dispersion relations.) Its energy dependence is an important test of Regge theory (ρ exchange). Its t-dependence yields information on flip vs. non-flip amplitudes. Results will be reported at London on this reaction as well as for $\pi^- p \to \eta n$ (A_2 exchange). These results will be quite significant.[14]

Turning to the subject of small angle inclusive scattering, I assume you are familiar with the published experiments from Fermilab and ISR on pp → pX at various t and x ranges.[15]

One of the most interesting experiments performed on pp → pX at small momentum transfers was[16] Exp. No. 14 (Columbia-Stony Brook). Since then, the apparatus has been moved to the ITA and renamed Exp. No. 221. The set-up there is illustrated in Fig. 23. The telescopes have been modified to include three solid state detectors of different thicknesses. This allows even better resolution in the range of momentum transfers, $0.011 < |t| < 0.244$ GeV^2. By running at the internal target area, the entire energy range of the main ring is accessible. The experiment accepts a wide range in missing mass, $1 < M_x^2 < 100$ GeV^2. with a good resolution of $\Delta M_x^2 \approx 0.7$ GeV^2, another nice feature of this experiment. Owing to experimental complications arising from moving to the ITA, the results have been delayed, but should be available soon. It will be interesting to see the energy dependence at fixed missing mass and to see how the turnover in t previously reported in Exp. No. 14 looks as a function of energy. This turnover is one of the most interesting aspects of the results, which have not been supported by the NAL BC data at 300 GeV/c.[17]

Another experiment on inclusives is Exp. No. 186 (Dubna (USSR), Rockefeller U., U. of Rochester and Fermilab) on deuteron scattering (dp → dX) using the gas jet at the internal target. The recoil deuteron

is detected in small spectrometer using solid state detectors (Fig. 24). By determining the recoil energy and angle of the deuteron, the momentum transfer t and missing mass M can be determined. The range of t accessable is about $0.035 < |t| < 0.1$ with a resolution of approximately 1%. The resolution in the missing mass is a function of the incident momentum, momentum transfer, and angular resolution ($\Delta\omega$ = 3 mrad). This experiment, another joint US-USSR collaboration, will report preliminary results at London, but I have little to present here. I have heard a seminar on this and can tell you some general features of the results.[18] First, on elastic scattering $dp \rightarrow dp$, there is evidence of shrinkage similar to pp elastic. On the inelastic cross section, $dp \rightarrow dX$, there appears to be little energy dependence (for M^2 out to 30 GeV^2) and the dependence on M^2 is consistent with $(M^2)^{-1}$. Thus, the data is dominated by a triple pomeron term. After taking out a factor of e^{26t} for the deuteron coupling to the pomeron, there appears to be no evidence for the turnover at small t indicated in Exp. No. 14. However, one should be cautious in comparing these results, since this is an experiment with deuterium, and we are looking for a small effect in a function which decreases rapidly with increasing t because of the deuteron "form factor" alone. The data I saw was quite preliminary and did not compell one to disbelieve Exp. No. 14. I found surprising the lack of energy dependence which, for large M^2, would be quite different from the results on $pp \rightarrow pX$ seen

in both Exp. No. 14 and the 30" Bubble Chamber. I would like to tell you briefly about some theoretical work being done with this data by V. Tsarev, a theoretist attached to the experiment. I believe his work is indicative of the sort of useful phenomenology which can be done as soon as the results become finalized and public. One can, in principle, take the results for elastic scattering and low missing mass inelastic scattering and evaluate the triple pomeron coupling from a finite missing mass sum rule (see Fig. 26). This is an interesting thing to do because one would like to understand duality for pomeron-proton scattering. A few years ago, it was suggested that, unlike hadronic total cross sections, resonances and background would contribute to the pomeron in pomeron hadron scattering.[19] This would mean, in particular, that the elastic amplitude would contribute to $G^{p}_{pp}(t)$ at $t \neq 0$.

Tsarev inserts the elastic and inelastic data into the left-handed side and obtains a fairly reasonable triple pomeron coupling. He finds in particular, the elastic contribution is essential for obtaining a reasonable $G^{p}_{pp}(t)$ coupling. If supported by the final data and analysis, this will be as good example of the sort of information which can be obtained from these experiments.[20]

This concludes my discussion of experiments bearing on diffraction. Another area of considerable theoretical interest and experimental activity concerns the reproduction of particles at large transverse momentum. I will speak first about hadron production.

In a substantial contribution to the London Conference,[21] Exp. No. 100 (Chicago-Princeton) summarizes their results for production near 90^{o} in the center of mass of $\pi^{\pm}$, $K^{\pm}$, p, $\bar{p}$, d, and $\bar{d}$ for protons on tungsten (W). The layout of the experiment is presented in Fig. 26. It is a single arm spectrometer with with 2 Cerenkov counters to permit simultaneous recording of π, K, and proton yields. Particles were detected over a wide range of momentum, from $p_{\perp} = 0.8$ to as large as 9 GeV/c. This corresponded to a change in the measured cross sections of 11 orders of magnitude! The cross section for π^{-} production per effective nucleon in W is shown in Fig. 27. Note that, at fixed $p_{\perp}$, the cross section rises with energy as had been noted already at the ISR[22] over a more limited momentum range. (The curves for π^{+} are essentially identical to these for π^{-}.) At fixed $x_{\perp} = 2p_{\perp}/\sqrt{s}$, the curves become very nearly parallel for $x_{\perp} > 0.4$, as can be seen in Fig. 28. This suggests a kind of scaling law, and, as indicated in that figure, the three energies can be fit well, for $x_{\perp} > 0.4$, by a form $s^{-5.4} \exp(-36\, x_{\perp})$. The quality of this scaling is demonstrated in Fig. 29, where the departure at smaller $x_{\perp}$ is also indicated. This power of 5.4 is greater than the power of 4.1 seen by the CCR collaboration[22] at smaller $x_{\perp}$. In the $x_{\perp}$ range where the data overlap ($0.1 < x_{\perp} < 0.35$), however, the π^{o} spectrum seen at the ISR agrees with the $\pi^{\pm}$ spectra seen at Fermilab. In fact, the "effective" power falloff does increase throughout the range from about 3 at $x_{\perp} = 0.1$

to about 5 at $x_\perp = 0.3$, giving an average falloff of 4 acclaimed by CCR.

The spectra for other particles can be most easily described by comparison with the pion spectra. In Fig. 30, we show the kaon spectra. The K^+ seems to show signs of scaling like the π^+, but K^- differs considerably from π^-. For the theoretical interpretation of all these results, I recommend to you the lectures of Professors Blankenbecler and Polkinghorne at this symposium. However, some qualitative insight into these results can be gleaned by classifying the produced hadrons in terms of the quark model. The initial pW state contains only u and d valence quarks. An outgoing pion contains one of these quarks plus an antiquark, (which is not among valence quarks) and thus may be thought of as "first-forbidden." An outgoing $K^+ = u\bar{s}$ is, like pions, first forbidden. A produced $K^- = s\bar{u}$ is doubly-forbidden, since neither of its two valence quarks occur in the initial state. This kind of structure may account for the difference between K^+ and K^- spectra. Similar remarks hold for the comparison of the production of protons and antiprotons. (Figure 31). The comparison of baryon spectra with meson spectra requires a detailed model. (See Prof. Blankenbecler's lecture.) Note also that deuterons (and antideuterons) are detected. These rates can be accounted for as a convolution of probabilities for producing a proton and neutron in the correct regions of phase space to combine to give a deuteron.

The interpretation of this data for particle physics is obscured somewhat by the fact that the experiment was performed with a W target, since it is difficult to know what the cross section would be for a proton on a nucleon. To partially remedy this, the same group performed measurements at 300 GeV with Ti and Be targets as well. For each value of $p_\perp$, the invariant cross section was compared with the Be rate,[23] as shown in Fig. 32. The dependence on atomic number A is described well by a simple power A^n, but the exponent n is seen to be a function of both particle type and transverse momentum. (Here's a good problem of nuclear physics!) However, above about $p_\perp = 3.5$ GeV, the exponent becomes independent of $p_\perp$ for pions of momentum greater than 3.5 GeV/c, leveling off at $n = 1.1$. (Figure 33). This means that the effective number of nucleons in W is the same throughout the region where it was claimed scaling holds. For smaller $p_\perp$, replotting the results by taking into account this variation of n with $p_\perp$ does not improve scaling.[24] The proton, antiproton, and kaon cross sections are steeper functions of $p_\perp$ than are pions. For further discussion of these data, I refer you to Ref. 23.

Another beautiful experiment on wide angle production involves the detection of the single photon spectrum at the Internal Target Area (Exp. No. 63A, Fermilab-Northern Illinois). Some early results have already been published,[25] and a great many more will be presented at the London Conference.[26] Carbon fibers were employed as a target and,

in addition, runs were performed with the gas jet to normalize the detectors. The layout is given in Fig. 34 and is fairly self-explanatory. Using the standard Sternheimer technique, the slope of the photon cross section is simply related to the π^o cross section (neglecting complications from the production of other particles giving photons, such as the η.) The kinematical range to be explored in this experiment is given by the curves shown in Fig. 35. The data I will show you comes from analyses at four laboratory angles, 65, 80, 100, and 120 mrad. At each angle, data are accumulated at several different energies along the acceleration ramp, viz., 51, 106, 201, 251 GeV/c,and for a wide range of momenta corresponding to 0.3 GeV/c $\leq p_\perp <$ 4.3 GeV/c. Thus the invariant cross section can be studied as a function of its three independent kinematical invariants, energy (s), outgoing momentum (p), and center of mass scattering angle (Θ). Rather than presenting you with the raw data, let me tell you their main conclusion. Over the observed range, the invariant cross section for π^o $E \frac{d\sigma}{d^3p}$ can be well represented as $g(p_\perp) f(x_R)$ where $p_\perp = p \sin\Theta$, $x_R = 2[p_\parallel^2 + p_\perp^2)/s]^{1/2} = p^*/p^*_{max}$. x_R is the function of total allowed momentum carried off by the pion may also obviously be written as $x_R = \sqrt{x_\parallel^2 + x_\perp^2}$ or simply related to the missing mass $\mathcal{M}^2 \approx (1 - x_R)S$. There is a great deal of content in this statement: (1) At fixed $p_\perp$ and x_R, the cross section is energy independent. (2) The dependence on $p_\perp$ and x_R factorizes. At each angle, the function $f(x_R)$ is determined independently, but it agrees well at all

four angles. It is given in Fig. 36 for 80 mrad. It is described roughly by a $(1-x_R)^4$ curve. Having determined $f(x_R)$, $g(p_\perp)$ can be determined and is displayed in Fig. 37 at 80 mrad. The solid curve in Fig. 37 is the function $(p_\perp^2 + 0.86)^{-4.5}$. A great deal more data exists than is shown here and even more is being taken at other angles. All together, the claim is impressive. At 90^o, $x_R = x_\perp$, yet I reported that Exp. No. 100 found scaling only for $x_\perp > 0.4$ which, because of luminosity limitations, is just out of reach for Exp. No. 63A. The confusion lies in the use of the word scaling. Experiment No. 100 showed that, at fixed $x_\perp$, the power falloff with energy was different at larger $x_\perp$, than at smaller $x_\perp$. This means that the functional form for $g(p_\perp)$ given above must change from $p_\perp^{-9.0}$ to $p_\perp^{-10.8}$ as $p_\perp$ increases beyond about 3.5. In the region of overlap, both experiments are compatible and, as noted earlier, agree with CCR results.[22] From the theoretical point of view, it had already been suggested[27] by proponents of the "constituent interchange model," that the invariant cross section would be a sum of terms of the form suggested by Exp. No. 63A. Consequently, it is perhaps not so surprising that, over a limited kinematical range, only one effective term works well. As indicated above, the $p_\perp$ dependence must change at larger $p_\perp$. Whether a sum of terms is preferred over a simpler, single term remains to be tested. I refer you again to Professor Blankenbecler's lecture for further discussion of this point as well as to Ref. 26 for comparisons with

other data.

Finally, let me turn to the direct production of leptons at large transverse momentum. Using their muon identifier (see Fig. 26), Exp. No. 100 (Chicago-Princeton) has detected muons which pass through their spectrometer. By running with no absorber or with either a tungsten or an iron absorber inserted into the spectrometer near the target, they could infer what proportion of the muons was due to production in the target itself. For details, I refer you to their recent preprint.[28] The effects of the absorbers can be calculated from the measured rate of hadronic production and known decay rates to muons. The results of their calculation compare beautifully with their observations, adding confidence to the claimed muon signal from their target. They measure the ratio of muons produced to pions produced at the same momentum. Their results are most simply summarized by the statement that the direct production of muons is a constant fraction (0.8×10^{-4}) of the pion yield (for both positive and negative muons) for transverse momenta between 1.5 and 5.4 GeV/c. The data are shown in Fig. 38. Since most hadrons have similar transverse momentum distributions) the fact that the muon signal tracks the pion cross section so closely suggests a hadronic source for the muons. This is reinforced by the independence of the muon/pion ratio for Be, Cu, and W targets, in spite of the fact that the yield of pions varies with atomic number and transverse

(Recall Figs. 32 and 33 and associated discussion). Estimates based on partons models of quark-antiquark annihilation[29] predict a much smaller muon signal than observed. (This is the dashed curve in Fig. 37). All these observations suggest that the muons come from the decay of some strongly interacting source. Looking at the leptonic branching ratios of hadrons, we find the vector mesons, especially the ϕ, are candidates for the muon signal. Estimates,[28] show that if the ρ and ϕ mesons are produced as copiously as pions, then the predicted ratio μ/π is 0.68, 0.46 and 0.33×10^{-4} at $p_\perp$ of 1.5, 3.0 and 4.5 GeV/c respectively, with the ϕ being the predominant contributor. I believe such a large cross section for ϕ production is unlikely. The ϕ is predominantly $s\bar{s}$ which, in the language used earlier, is a "doubly-forbidden" reaction. Thus, we would expect the ϕ production to be comparable to K^- production, about 10% of the pion cross section. Although heavier mesons may also contribute, their branching ratio to muons is presumably less than the ϕ. Consequently, we believe that a theoretical puzzle is shaping up here, for the observed muon signal is perhaps an order of magnitude larger than expected.

Two other experiments have detected the direct production of leptons. Although their results will be presented in London, they were not quite ready to be quoted at the time I left. One of them, Exp. No 70 (Columbia-Fermilab), is in the Proton Area. A schematic of their layout is shown in Figs. 39a and 39b. Having both a magnet

and a lead glass shower counter, they can do both an energy and momentum analysis of the produced lepton. While I have no graphs to show you, I can tell you that their muon signal, for both charges, agrees well with the data[28] from Exp. No. 100. They also have identified electrons and positrons, whose cross sections are nearly the same as for the muons.[30]

A third experiment, Exp. No. 184 (Chicago-Harvard-Pennsylvania-Wisconsin), operates in the Internal Target Area in a vertical plane underneath the beam pipe. Their set-up is shown in Fig. 40. Nominally, the experiment is a search for weird new particles. Having magnets, Cerenkov counters, and lead glass makes possible momentum measurements as well as particle identification. Suffering from the disadvantage of luminosity, they are more limited than Exp. No. 70 or Exp. No. 100 in the range of momenta which can be covered. On the other hand, working in the ITA, they have the advantage of easily studying the energy dependence of production. Preliminary results will be available shortly and are eagerly awaited.[31]

ACKNOWLEDGMENTS

It is obvious that, without the cooperation of at least one person from each of the experiments discussed, my success as a conduit for data from Fermilab to this Symposium would have been considerably limited. While I am indebted to a great many experimentalists for conversations, I have tried to acknowledge in the footnotes those who

contributed directly to this review. In addition, I enjoyed lengthy conversations with G. Giacomelli, who was preparing a similar review at the same time. I apologize in advance to those whom I inadvertantly failed to mention or whose experiments were omitted. Come see me.

ADDENDUM

In an effort to make this report as up-to-date as possible, I will indicate some of the relevant information which has become available since the Symposium:

1) Data from Exp. No. 4 has appeared in M. J. Longo et al., University of Michigan Preprint HE 74-22, June 1974. The energy dependence of the neutron-proton cross section reported here is much less dramatic than indicated by the preliminary data shown in Fig. 47.

2) Data from Exp. No. 70 on hadron and lepton production at large transverse momentum appears in J. A. Appel et al., NAL-Pub-74/70-EXP, 7100.070 and NAL-Pub-74/41-EXP, 7100.070 (submitted to Phys. Rev. Letters).

3) Data from Exp. No. 184 on direct muon production was reported in London in a paper by D. Bintinger et al. Where they overlap, these results agree with Exp. No. 100 and Exp. No. 70. In addition, they report essentially no energy dependence of the muon/pion ratio.

4) Elastic scattering cross sections from Exp. No. 7 were presented in London and are available in C. W. Akerlof et al., University of Michigan Preprint UM HE 74-20.

5) Although I have no reference, I understand that Exp. No. 21 (Caltech-Fermilab) reported at London the observation of neutral currents in neutrino and antineutrino interactions.

6) Preliminary analysis from Exp. No. 221 (Columbia-Stony Brook) does not show any forward dip in $pp \rightarrow pX$, for the missing mass range where a turnover had been previously reported[13] in the t distribution. Other preliminary data from Exp. No. 221 support the M^{-3} dependence claimed previously.[13]

REFERENCES

[1] J. Whitmore, "Experimental Results on Strong Interactions in the NAL Hydrogen Bubble Chamber," NAL-Pub-73/70-EXP (submitted to Physics Reports).

[2] I would like to thank P. Limon for a lecture on the muon beamline.

[3] E. D. Bloom, "Recent Results on Inclusive Electron Scattering from Hydrogen, Deuterium, and other Nuclei," in Experiments on High Energy Particle Collisions--1973 (Vanderbilt Conference), R. S. Panvini (ed.), AIP Conference Proceedings No. 12, American Institute of Physics, N. Y., 1973.

[4] Conversations about Exp. No. 26 with W. Chen and L. Hand were invaluable to me.

[5] I appreciate L. Mo's bringing up to date concerning the status of this experiment.

[6] The data is available in the report from Exp. No. 104 presented at the London Conference and papers submitted to Phys. Rev. Letters.

[7] D. P. Sidhu and C. Quigg, Phys. Rev. D7, 755 (1973); C. Quigg and L.-L. Wang, Phys. Letters 43B, 314 (1973).

[8] S. P. Denisov, et al., Nucl. Phys. B65, 1 (1973).

[9] I especially profitted from discussions with W. Baker, R. Rubinstein,

and G. Giacomelli about Exp. No. 104.

[10] pp total cross section, H. R. Gustafson, et al., Phys. Rev. Letters 32, 441 (1974).

[11] I appreciate M. Longo providing me with this preliminary data as well as Figs. 46 and 47.

[12] I enjoyed talking with A. Weitsch and A. Brenner regarding Exp. No. 96 and thank the latter for providing me with Fig. 22.

[13] Conversations with D. Jovanovic about Exp. No. 7 have been both informative and entertaining.

[14] As Exp. No. 111 has progressed, discussions with A. Tollestrup and R. Walker have been very interesting.

[15] For a review of data and its implications for triple-Regge analyses, see R. D. Field and G. C. Fox, California Institute of Technology, Preprint CALT-68-434.

[16] S. Childress et al., Phys. Rev. Letters 32, 389 (1974) and 633 (E), (1974). See also J. Lee-Franzini in High-Energy Collisions, 1974 (Stony Brook), C. Quigg (ed.), American Institute of Physics, NY, 1973, pp. 147-179.

[17] I would like to thank the members of the Columbia-Stony Brook group (especially Frank Bletzacker) for providing me with a detailed statement on the status of Exp. 221.

[18]In addition to his seminar, D. Goulianos helped me to obtain some perspective about these results.

[19]M. B. Einhorn, M. B. Green, and M. A. Virasoro, Phys. Rev. D7, 102 (1973).

[20]I would like to express my thanks to V. Tsarev for telling me about his work.

[21]J. W. Cronin, et al., "Production of Hadrons with Large Transverse Momentum at 200, 300 and 400 GeV," paper presented in Session A_3 of the XVII International Conference on High Energy Physics, Imperial College, London, 1-10 July 1974.

[22]F. W. Busser et al., Phys. Letters 46B, 471 (1974).

[23]J. W. Cronin et al., "Atomic Number Dependence of Hadron Production at Large Transverse Momentum in 300 GeV Proton-Nucleus Collisions," paper presented in Session A_3 of London Conference.

[24]My thanks extend to J. W. Cronin for this information as well as for other discussions concerning these results. In addition, I have enjoyed conversations with H. J. Frisch about their experiment.

[25]D. C. Carey et al., Phys. Rev. Letters 32, 24 (1974).

[26]Some of this data and analysis is contained in two recent Fermilab preprints: D. C. Carey et al., NAL-Pub-74/48-EXP, 7100.063, May 1974 and NAL-Pub-74/49-THY/EXP, 7100.063, May 1974.

[27]R. Blankenbecler and S. J. Brodsky, SLAC-Pub-1430 (T/E), May 1974 and references therein.

[28]J. W. Cronin et al., Enrico Fermi Institute Preprint EFI-74/24.

[29]G. R. Farrar, California Institute of Technology Preprint CALT-68-422.

[30]I would like to thank T. Yamanouchi for providing me with the information reported here. I have also enjoyed conversations with B. Brown and L. Lederman.

[31]I am indebted to P. Wanderer and R. Imlay for several conversations about their experiments.

FIGURE CAPTIONS

Fig. 1 Some particle searches performed at Fermilab.

Fig. 2 Schematic of muon beam line

Fig. 3 (a) Kinematics of deep inelastic lepton scattering and Bjorken's scaling hypothesis.

(b) Scale transformation.

Fig. 4 Kinematical range available now at Fermilab.

Fig. 5 Illustrating scaling of the apparatus.

Fig. 6 Plot of the ratio R of observed rate to a Monte Carlo simulation based on SLAC structure functions.

Fig. 7 Schematic of Muon 98.

Fig. 8 A more detailed description of the apparatus for Muon 98.

Fig. 9 Layout for Exp. No. 104, hadron total cross sections.

Fig. 10 Preliminary results from Exp. No. 104: pp and $\bar{p}p$ total cross sections.

Fig. 11 $\pi^{\pm}p$ total cross sections.

Fig. 12 $K^{\pm}p$ total cross sections.

Fig. 13 pd and $\bar{p}d$ total cross sections.

Fig. 14 $\pi^{\pm}d$ total cross sections.

Fig. 15 $K^{\pm}d$ total cross sections.

Fig. 16 Differences of proton total cross sections: Negative minus positive.

Fig. 17 Differences of deuteron total cross sections: Negative minus positive.

Fig. 18 Layout for Exp. No. 4--neutron total cross sections.

Fig. 19 Preliminary results from Exp. No. 4 for the np total cross section.

Fig. 20 Preliminary results from Exp. No. 4 for the nd total cross section.

Fig. 21 pp differential cross section at very small t from Exp. No. 36. Taken from V. Bartenev et al., Phys. Rev. Letters 31, 1367 (1973).

Fig. 22 Detailed schematic of the Single Arm Spectrometer Facility.

Fig. 23 Schematic diagram for Exp. No. 221.

Fig. 24 Schematic diagram of set up for Exp. No. 186.

Fig. 25 Finite missing mass sum rules for pomeron-particle scattering.

Fig. 26 Single arm spectrometer for Exp. No. 100.

Fig. 27 Invariant cross section for $pW \rightarrow \pi^- X$, plotted vs. $p_\perp$, at per nucleon center of mass energies of 19.4, 23.8, and 27.4 GeV.

Fig. 28 Data as in Fig. 27, plotted vs. $x_\perp$.

Fig. 29 Test of "scaling" in $x_\perp$ for $pW \rightarrow \pi^- X$.

Fig. 30 Ratios of kaons to pions of like charge.

Fig. 31 Ratios of protons (antiprotons) and deuterons (antideuterons)

(antideuterons) to pions of like charge.

Fig. 32 Comparison of production of hadrons at 300 GeV/c from three nuclear targets, Be, Ti, and W.

Fig. 33 Effective exponent n as function of $p_\perp$ for production of pions.

Fig. 34 Schematic of Exp. No. 63A.

Fig. 35 Kinematic range accessible to Exp. No. 63A.

Fig. 36 The function $f(x_R)$ determined at 80 mrad. The solid line is $(1-x_R)^4$.

Fig. 37 The function $g(p_\perp)$ determined at 80 mrad. The solid curve is $(p_\perp^2 + 0.86)^{-4.5}$.

Fig. 38 Invariant cross section for direct production of muons.

Fig. 39 Schematic description of Exp. No. 70.

Fig. 40 Schematic diagram of apparatus for Exp. No. 184.

PARTICLE SEARCHES

Exp. No. 100 (Chicago-Princeton) Search for Massive Penetrating Particles EFI-74-29.

Exp. No. 76 (Fermilab) Search for Magnetic Monopoles NAL-Pub-73/51-EXP, 7100.076.

Exp. No. 75 (Cornell-NYU-Fermilab) A Search for Fractionally Charged Quarks, NAL-Pub-74/25-EXP, 7100.075.

Exp. No. 96 (Single Arm Spectrometer Facility Group) Search for Heavy Mass Particles and Antideuteron Flux Produced by 300 GeV Protons on Beryllium NAL-73/83-EXP, 7100.096.

Exp. No. 21 (Caltech-Fermilab) A Lower Bound on the Intermediate Vector Boson Mass, Phys. Rev. Letters 31 (1973) 180.

Exp. No. 21A (Caltech-Fermilab) Mass Limit on a Positively Charged Heavy Lepton, Phys. Rev. Letters 31, (1973) 410.

Figure 1

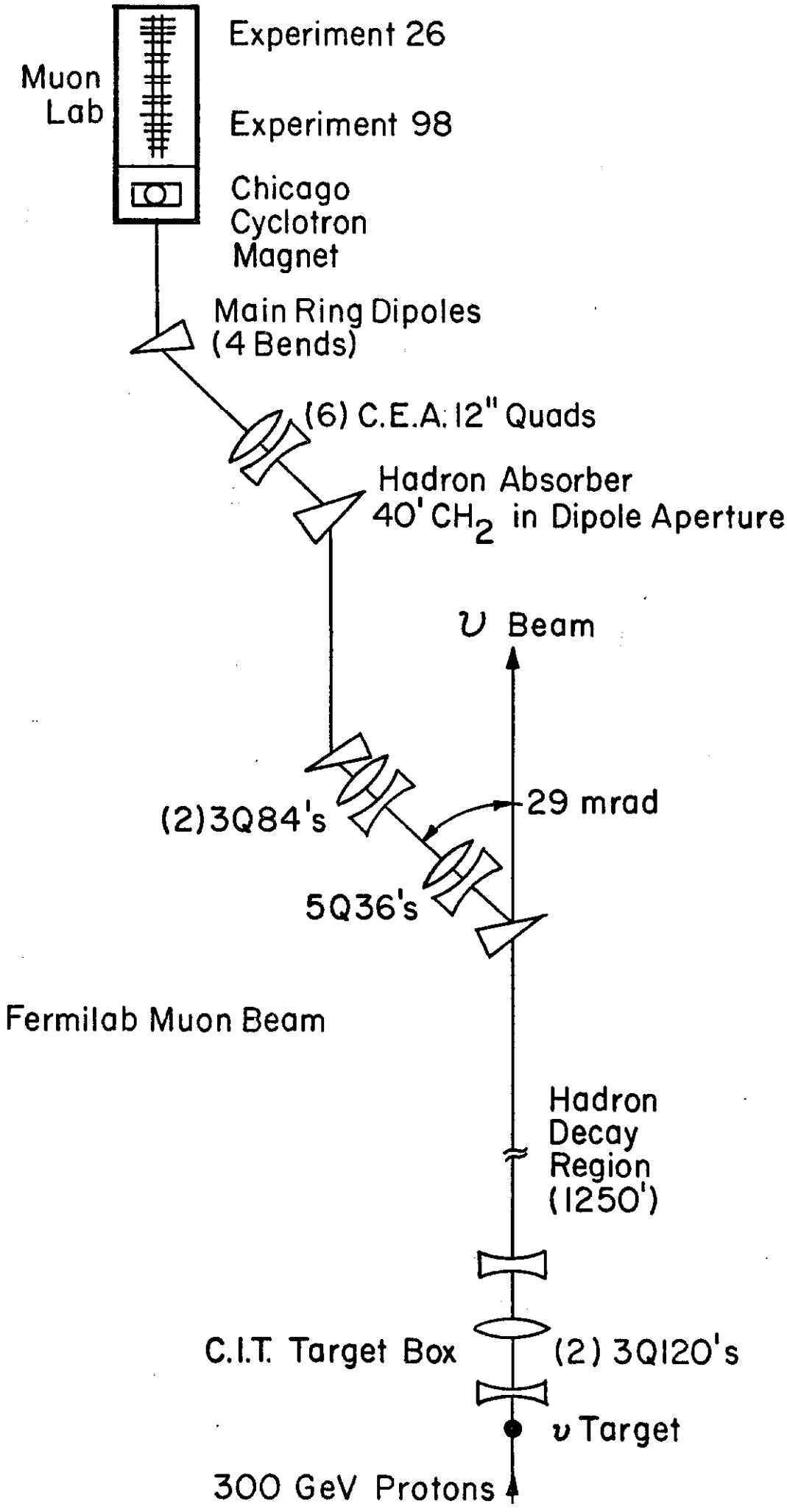
Muon Lab
Experiment 26
Experiment 98
Chicago Cyclotron Magnet
Main Ring Dipoles (4 Bends)
(6) C.E.A. 12" Quads
Hadron Absorber 40' CH_2 in Dipole Aperture
υ Beam
(2)3Q84's
29 mrad
5Q36's
Fermilab Muon Beam
Hadron Decay Region (1250')
C.I.T. Target Box
(2) 3Q120's
ν Target
300 GeV Protons

Figure 2

Kinematics of Deep Inelastic Lepton Scattering In Laboratory Frame

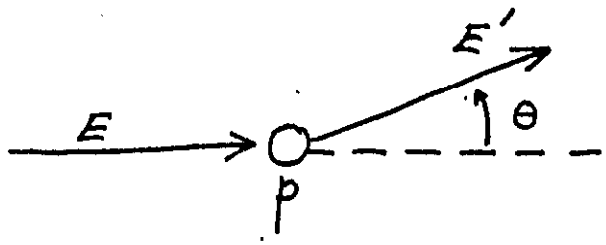

$$\nu = E - E'$$

$$Q^2 = 4EE' \sin^2 \frac{\theta}{2}$$

$$x = \frac{Q^2}{2M\nu}$$

$$\frac{d\sigma}{dE' d\Omega} = \left(\frac{\alpha}{2E \sin^2 \frac{\theta}{2}}\right)^2 \left[W_2 + (2W_1 - W_2)\sin^2 \frac{\theta}{2}\right]$$

Bjorken Scaling $\nu \to \infty$ for fixed x

$$\nu W_2(\nu, x) \to F_2(x)$$

$$W_1(\nu, x) \to F_1(x)$$

Figure 3(a)

Scale Transformation:

$$E \to \lambda E$$

$$E' \to \lambda E'$$

$$\sin \frac{\theta}{2} \to \frac{1}{\sqrt{\lambda}} \sin \frac{\theta}{2}$$

Also scale targets, separations, magnetic field, etc., implies:

$$\nu \to \lambda \nu, \qquad Q^2 \to \lambda Q^2, \qquad \text{fixed } x$$

Figure 3(b)

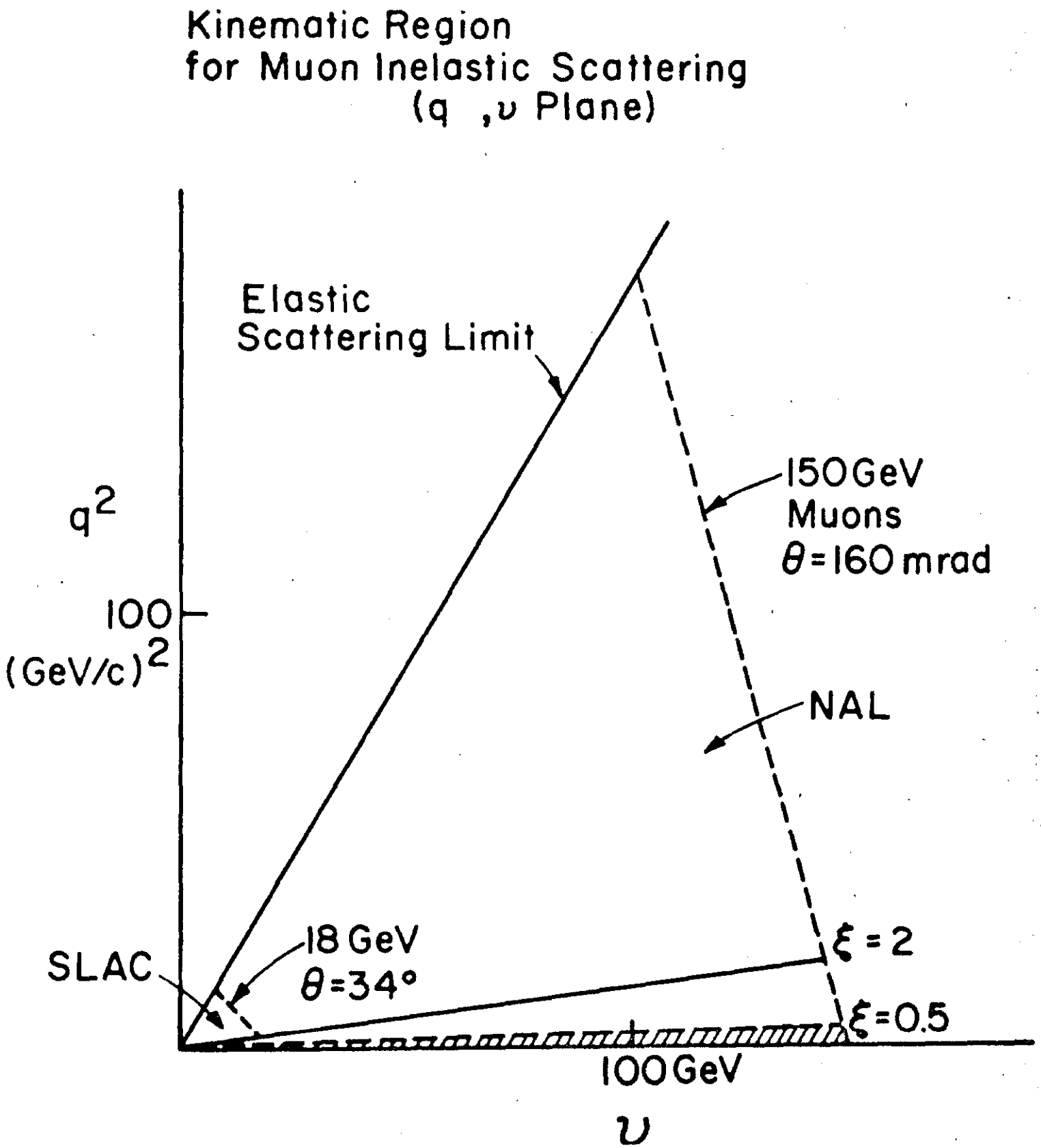
Kinematic Region
for Muon Inelastic Scattering
(q ,υ Plane)
Elastic
Scattering Limit
150 GeV
Muons
θ=160 mrad
NAL
18 GeV
θ=34°
SLAC
ξ = 2
ξ=0.5
100 GeV
q²
100
(GeV/c)²
υ

Fig. 4

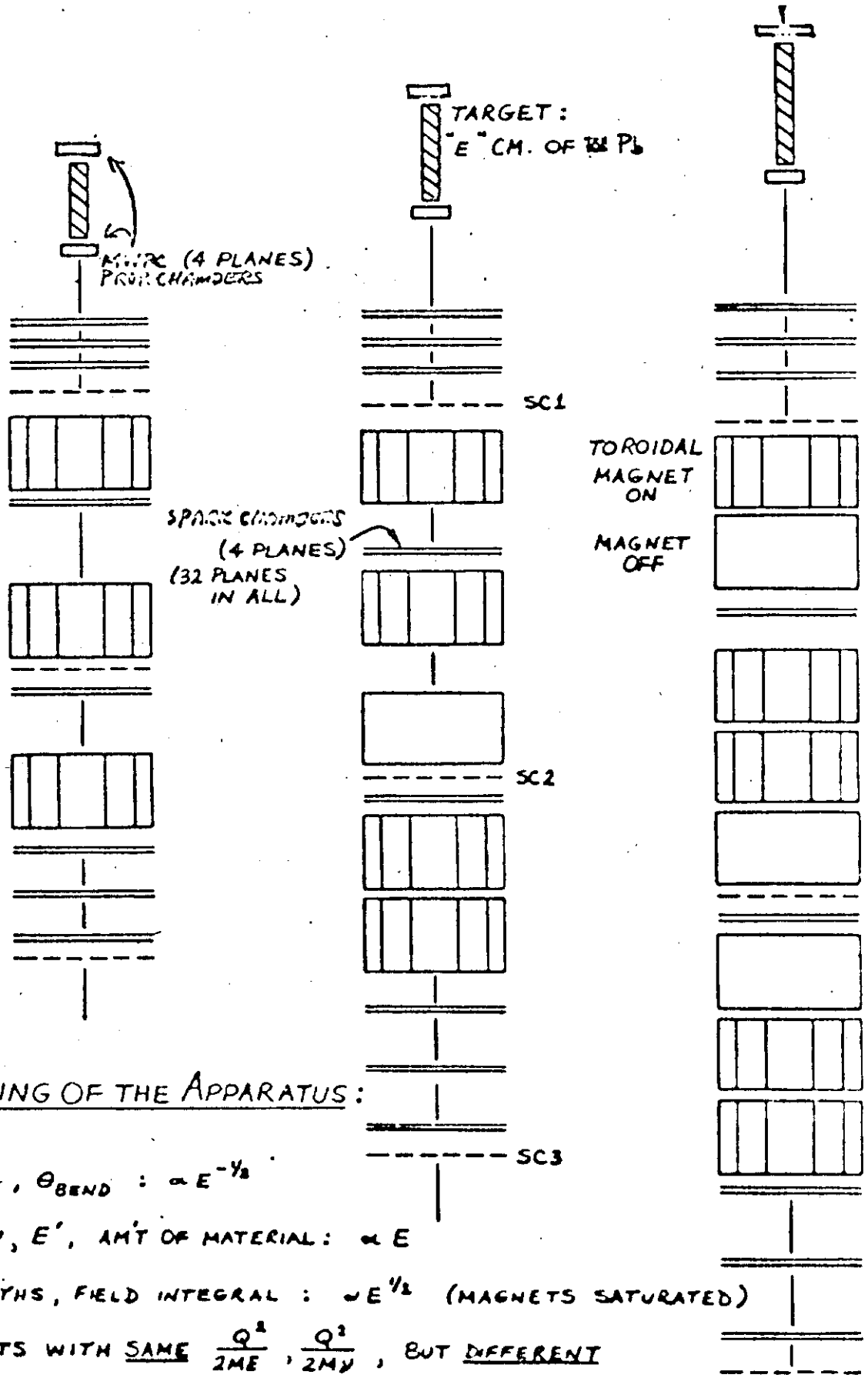

SCALING OF THE APPARATUS:

θ_{SCAT}, θ_{BEND} : $\propto E^{-1/2}$

Q^2, ν, E', AM'T OF MATERIAL: $\propto E$

LENGTHS, FIELD INTEGRAL : $\propto E^{1/2}$ (MAGNETS SATURATED)

EVENTS WITH SAME $\frac{Q^2}{2ME}$, $\frac{Q^2}{2M\nu}$, BUT DIFFERENT

Q^2 AND E, INTERSECT DETECTORS AT IDENTICAL XY COORDINATES

Fig. 5

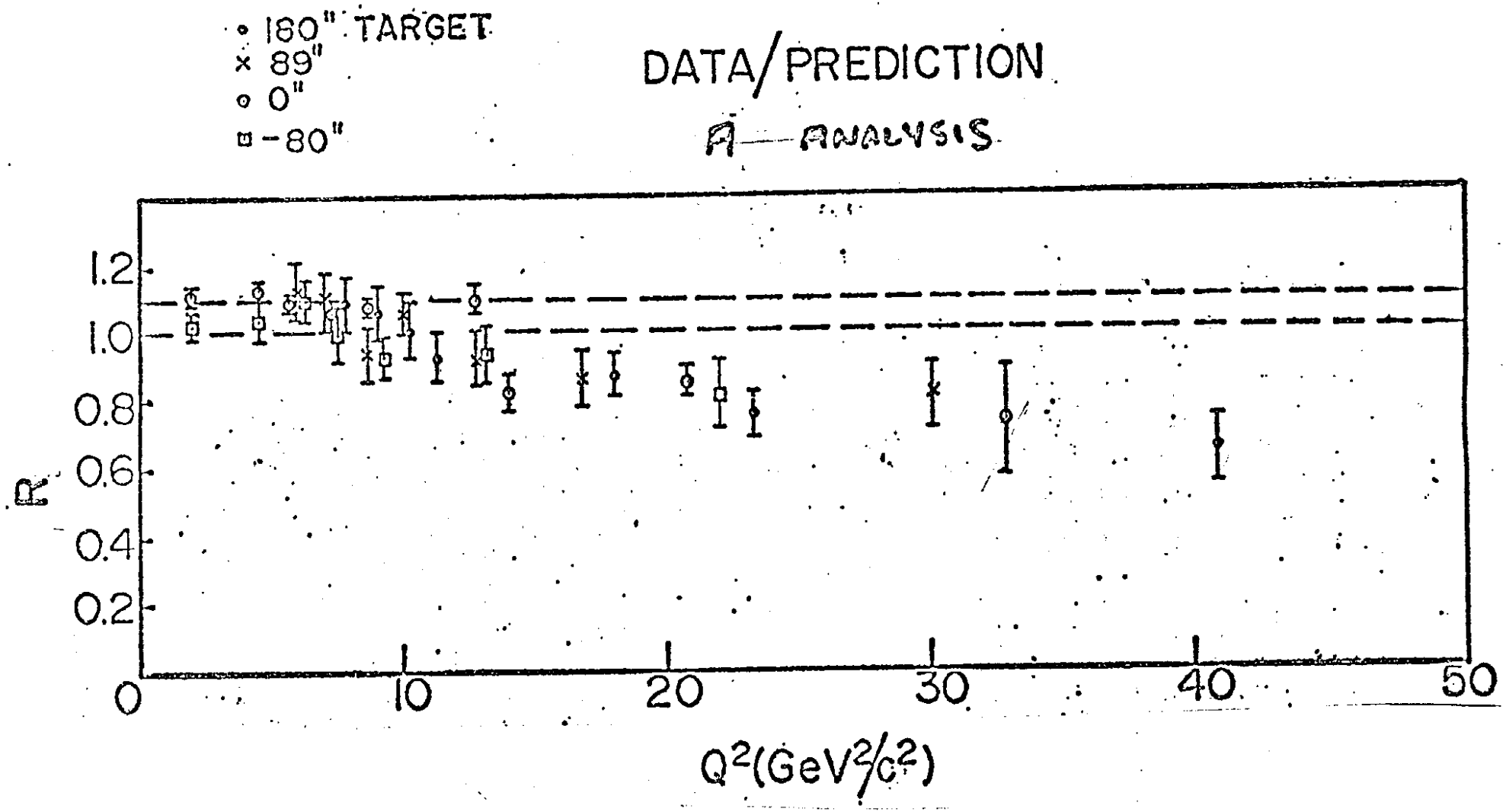
180" TARGET
89"
0"
-80"
DATA/PREDICTION
A — ANALYSIS
1.2
1.0
0.8
0.6
0.4
0.2
0
10
20
30
40
50
Q²(GeV²/c²)

Fig. 6

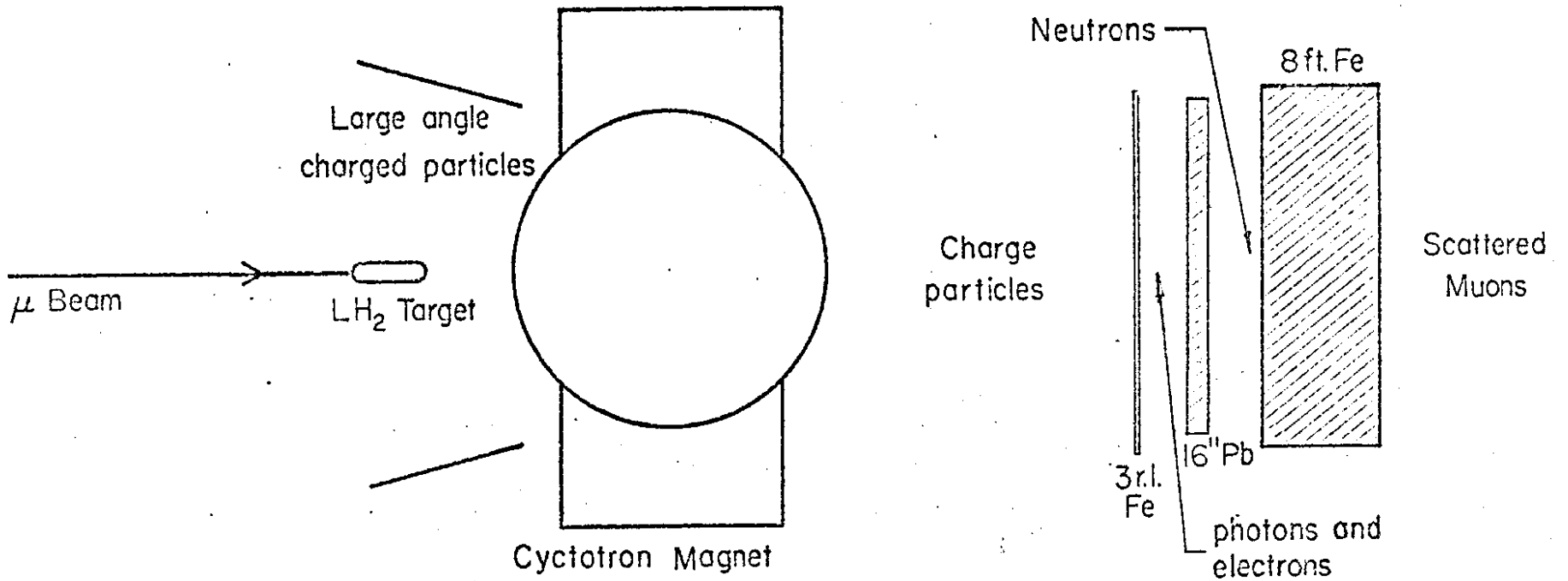
Large angle
charged particles
μ Beam
LH2 Target
Cyctotron Magnet
Neutrons
8 ft. Fe
Charge
particles
Scattered
Muons
3r.l.
Fe
16" Pb
photons and
electrons

Fig. 7

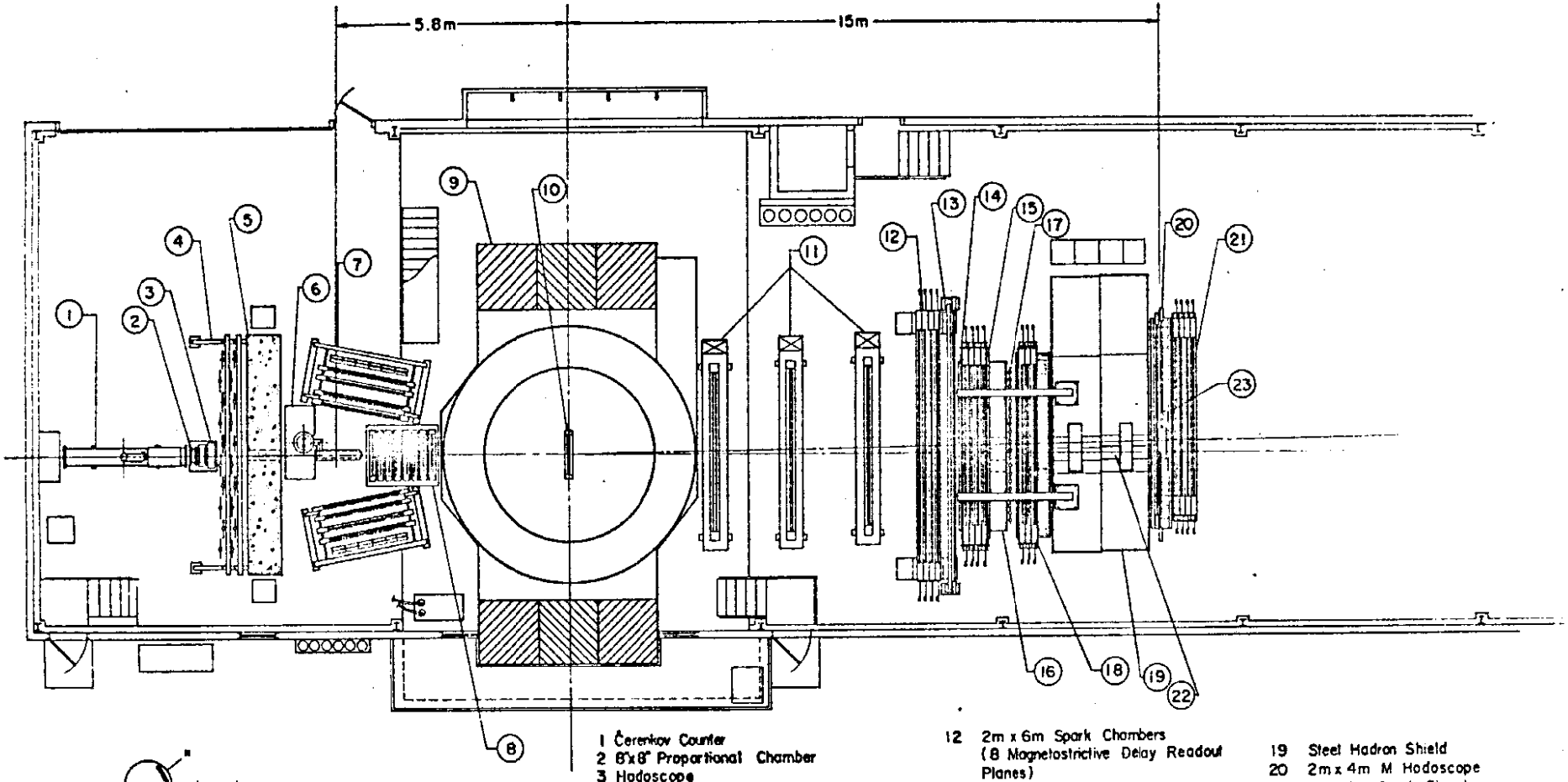
5.8m
15m
N (project)
0 1 10
Scale in Feet
1 Cerenkov Counter
2 8"x8" Proportional Chamber
3 Hodoscope
4 Halo Veto Counter
5 Backward Scattering Shield
6 Liquid H_2 Target (1m Long)
7 Spark Chambers & Time of Flight System
8 8 - 1m x 1m Proportional Chambers
9 Cyclotron Magnet (4.3m dia. Poletip)
10 1m x 1m Proportional Chamber
11 3-2m x 4m Spark Chamber
4 Shift Readout Planes / Chamber
12 2m x 6m Spark Chambers
(8 Magnetostrictive Delay Readout Planes)
13 2m x 6m G Hodoscope
14 2m x 6m x 2" Steel Plate
15 2m x 4m Spark Chambers
(8 Magnetostrictive Delay Line Readout Planes)
16 2m x 4m x 40.6cm Pb Absorber
17 2m x 4m H Hodoscope
18 2m x 4m Spark Chambers
(6 Magnetostrictive Delay Line Readout Planes)
19 Steel Hadron Shield
20 2m x 4m M Hodoscope
21 2m x 4m Spark Chambers
(8 Magnetostrictive Delay Line Readout Planes)
22 Removable Shutters
23 N Hodoscope

Fig. 8

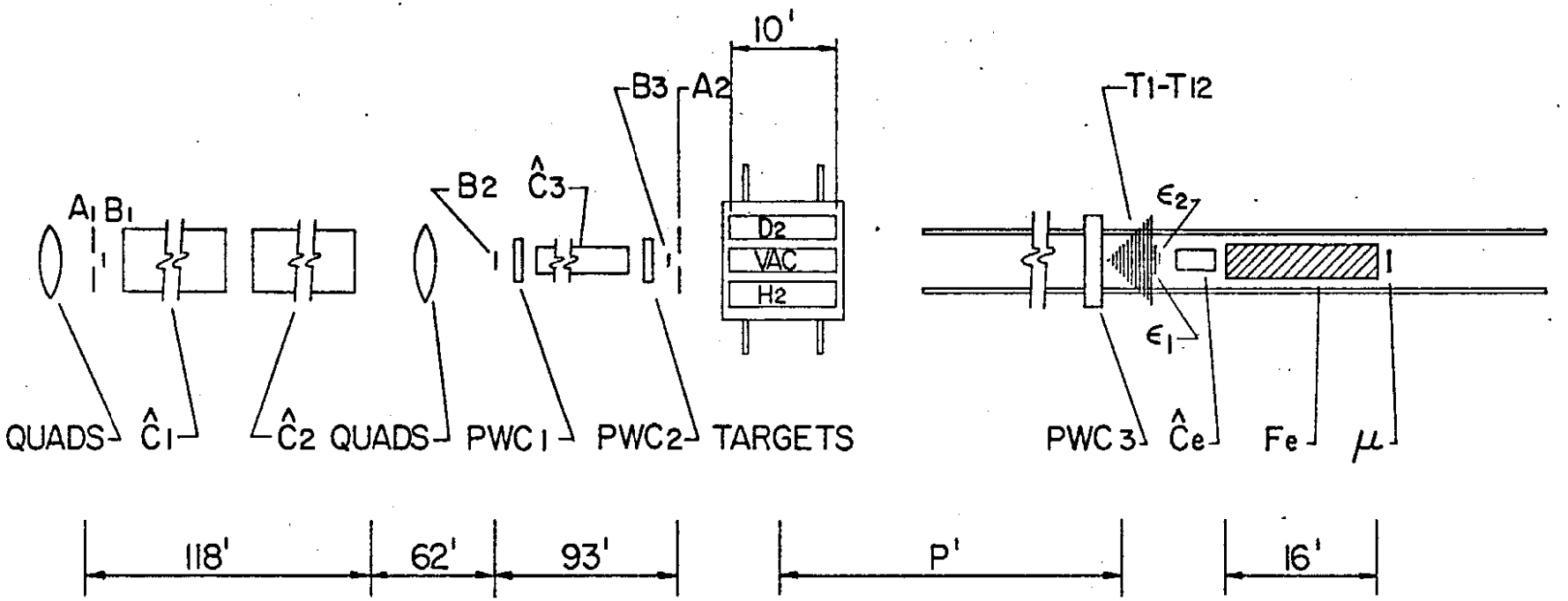

TOTAL CROSS SECTION EXPERIMENT

Fig. 9

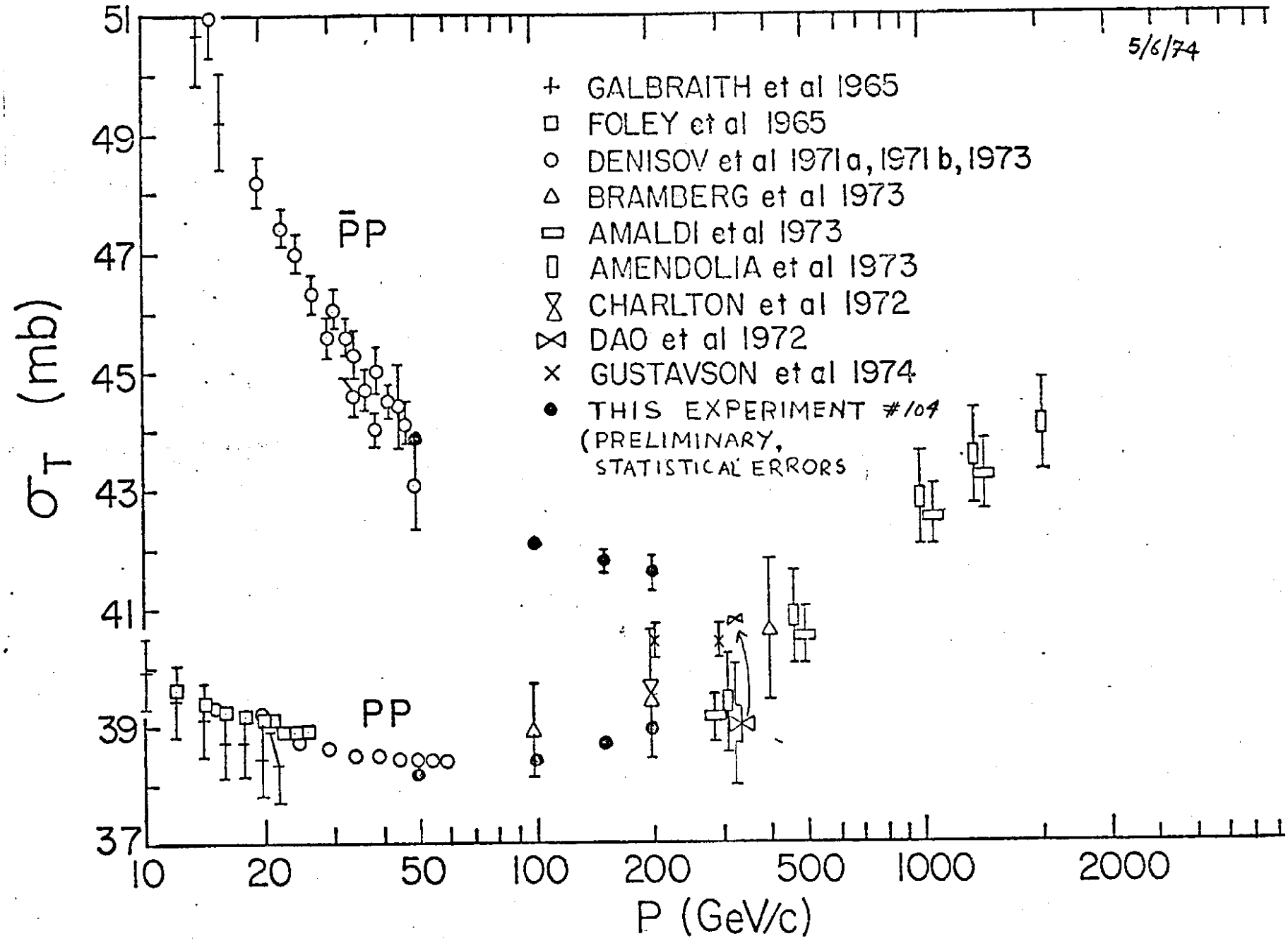
5/6/74
GALBRAITH et al 1965
FOLEY et al 1965
DENISOV et al 1971a, 1971b, 1973
BRAMBERG et al 1973
AMALDI et al 1973
AMENDOLIA et al 1973
CHARLTON et al 1972
DAO et al 1972
GUSTAVSON et al 1974
THIS EXPERIMENT #104
(PRELIMINARY,
STATISTICAL ERRORS
$\bar{P}P$
PP
σ_T (mb)
P (GeV/c)
51
49
47
45
43
41
39
37
10
20
50
100
200
500
1000
2000

Fig. 10

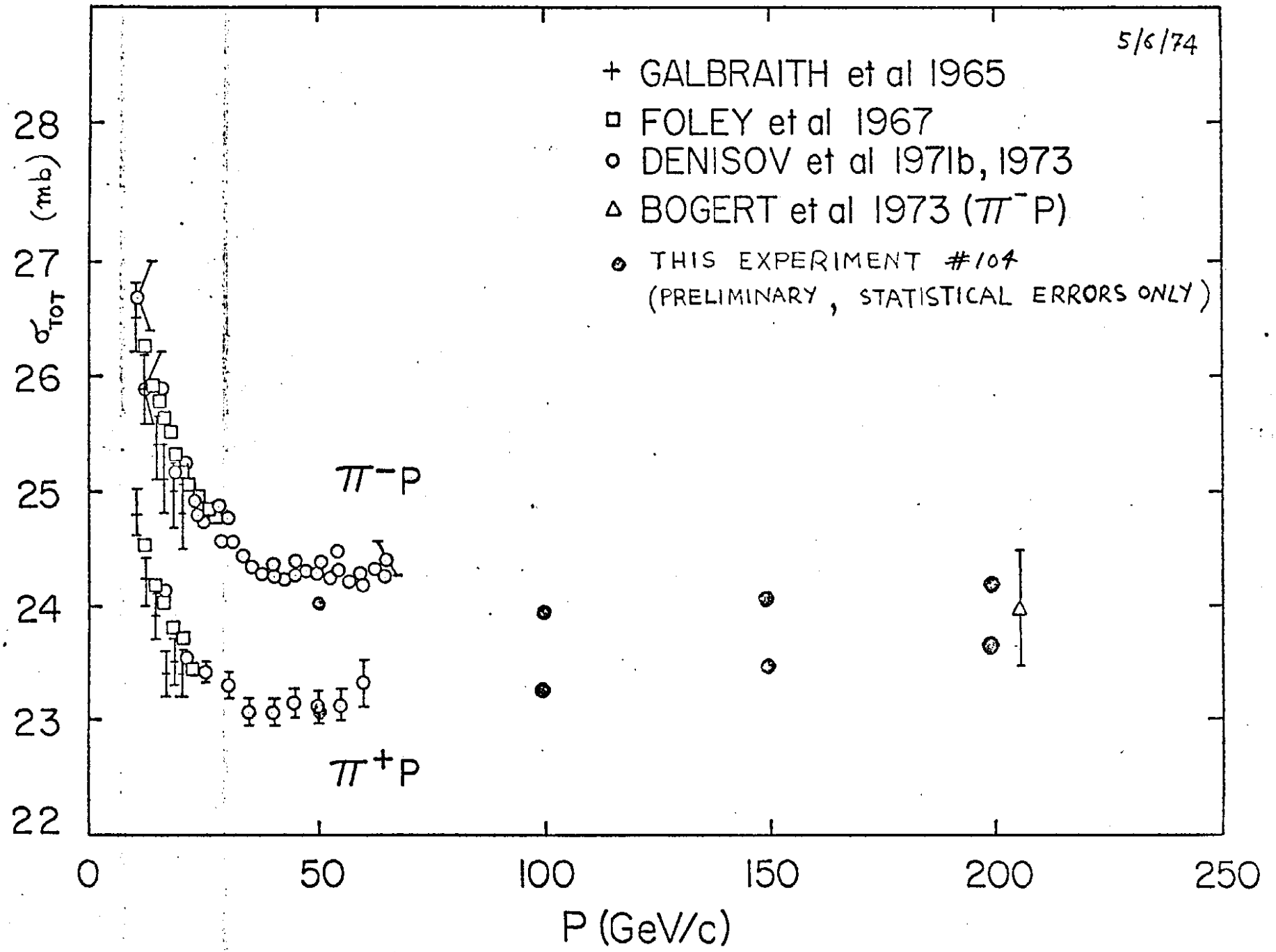
5/6/74
+ GALBRAITH et al 1965
□ FOLEY et al 1967
○ DENISOV et al 1971b, 1973
△ BOGERT et al 1973 (π⁻P)
⊙ THIS EXPERIMENT #104
(PRELIMINARY, STATISTICAL ERRORS ONLY)
σTOT (mb)
28
27
26
25
24
23
22
π⁻P
π⁺P
0
50
100
150
200
250
P (GeV/c)

Fig. 11

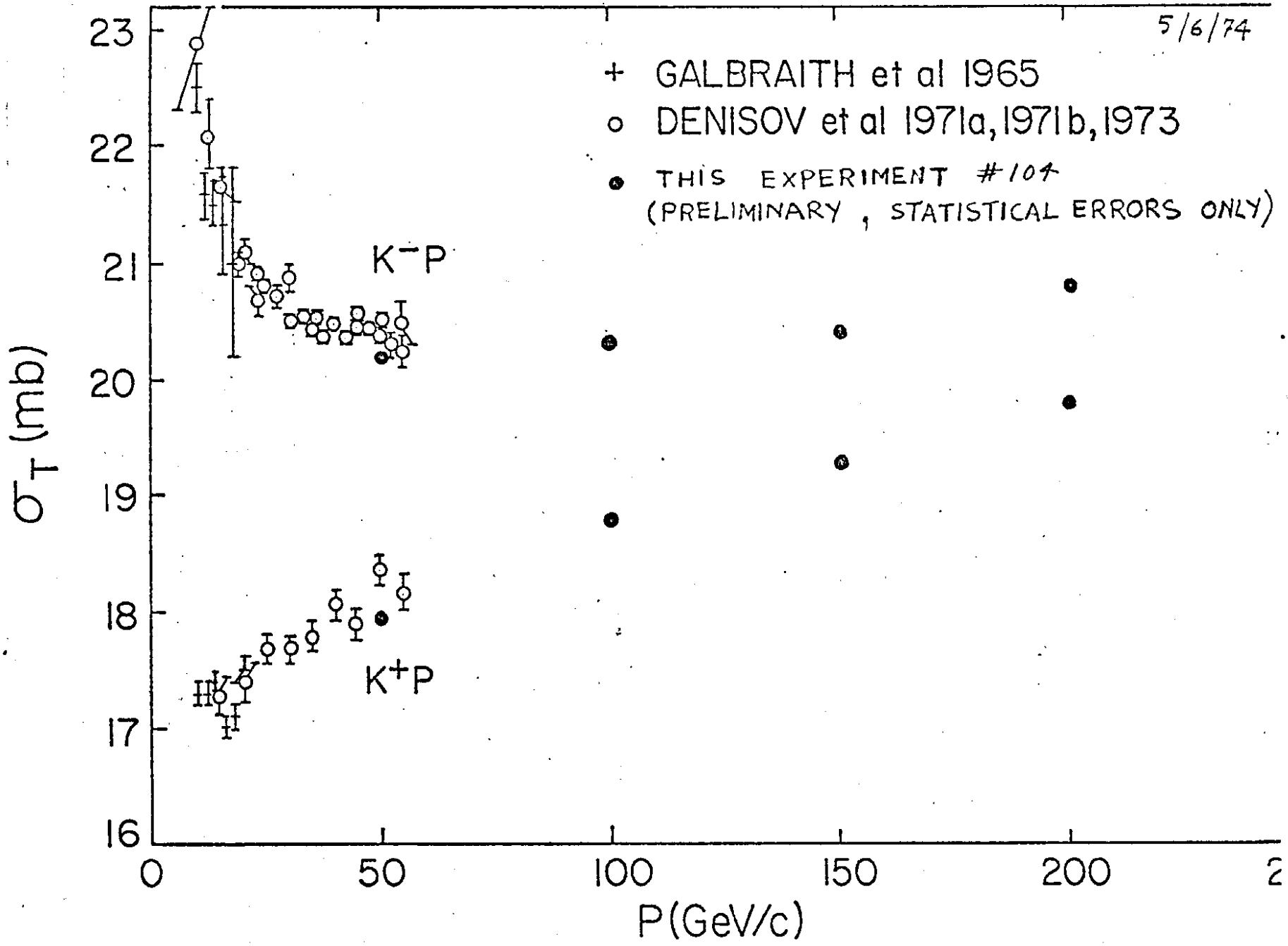
5/6/74
+ GALBRAITH et al 1965
o DENISOV et al 1971a, 1971b, 1973
● THIS EXPERIMENT #104
(PRELIMINARY , STATISTICAL ERRORS ONLY)
K⁻P
K⁺P
σT (mb)
P(GeV/c)
23
22
21
20
19
18
17
16
0
50
100
150
200

Fig. 12

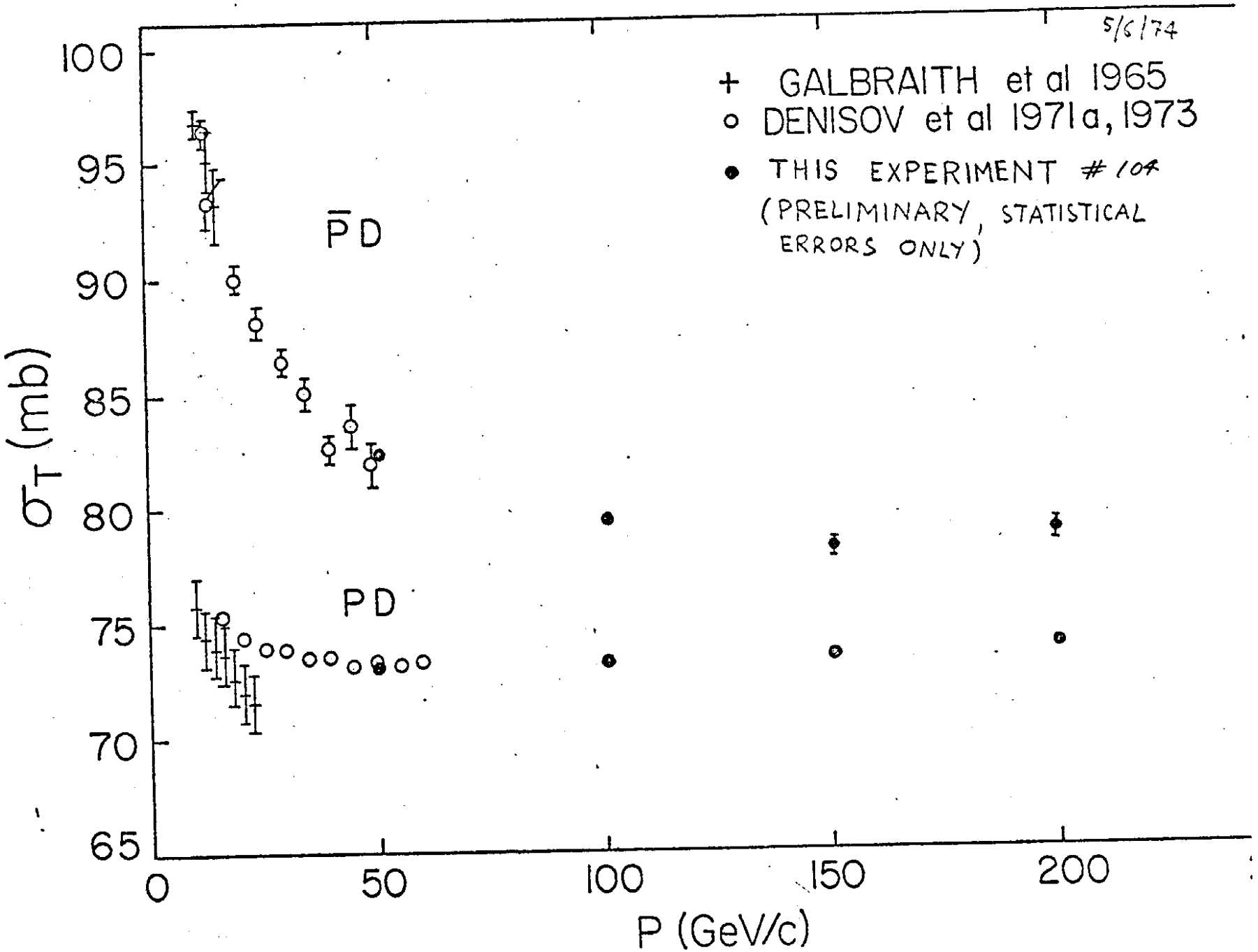
5/6/74
+ GALBRAITH et al 1965
o DENISOV et al 1971a, 1973
• THIS EXPERIMENT #104
(PRELIMINARY, STATISTICAL ERRORS ONLY)
P̄D
PD
σT (mb)
P (GeV/c)
100
95
90
85
80
75
70
65
0
50
100
150
200

Fig. 13

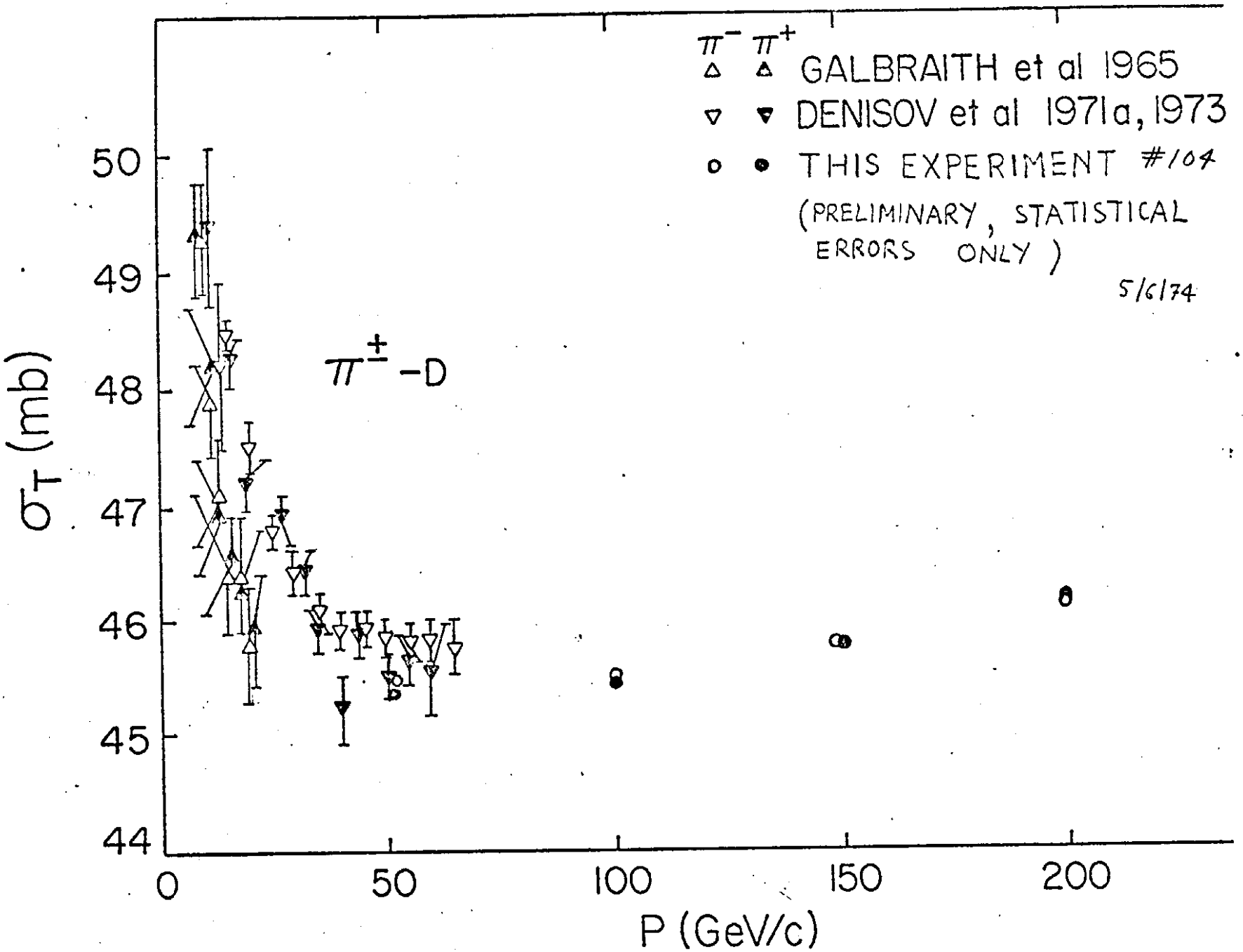
π^- π^+
GALBRAITH et al 1965
DENISOV et al 1971a, 1973
THIS EXPERIMENT #104
(PRELIMINARY, STATISTICAL ERRORS ONLY)
5/6/74
$\pi^\pm$-D
σ_T (mb)
50
49
48
47
46
45
44
0
50
100
150
200
P (GeV/c)

Fig. 14

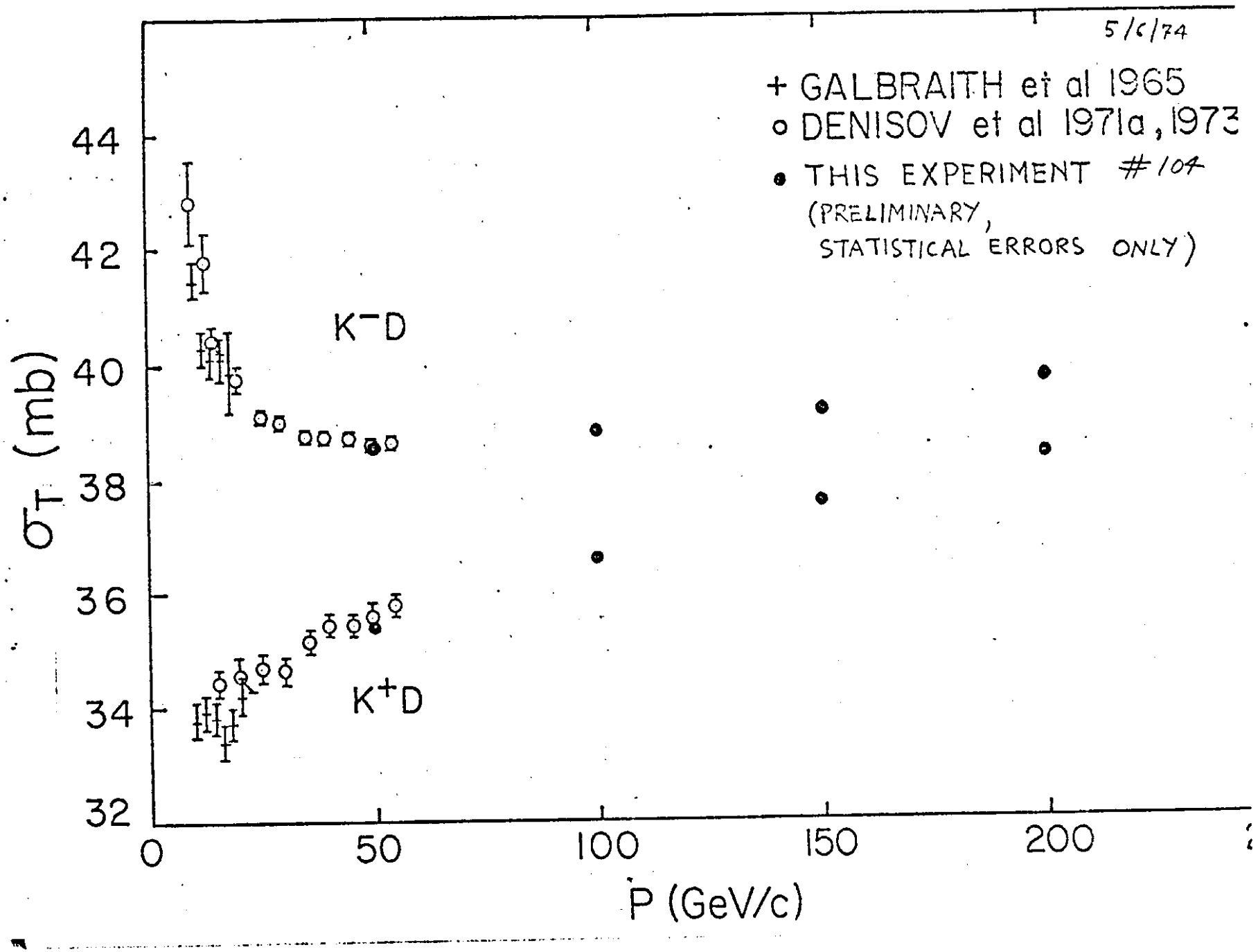
5/c/74
+ GALBRAITH et al 1965
o DENISOV et al 1971a, 1973
• THIS EXPERIMENT #104
(PRELIMINARY,
STATISTICAL ERRORS ONLY)
K⁻D
K⁺D
σT (mb)
P (GeV/c)
44
42
40
38
36
34
32
0
50
100
150
200

Fig. 15

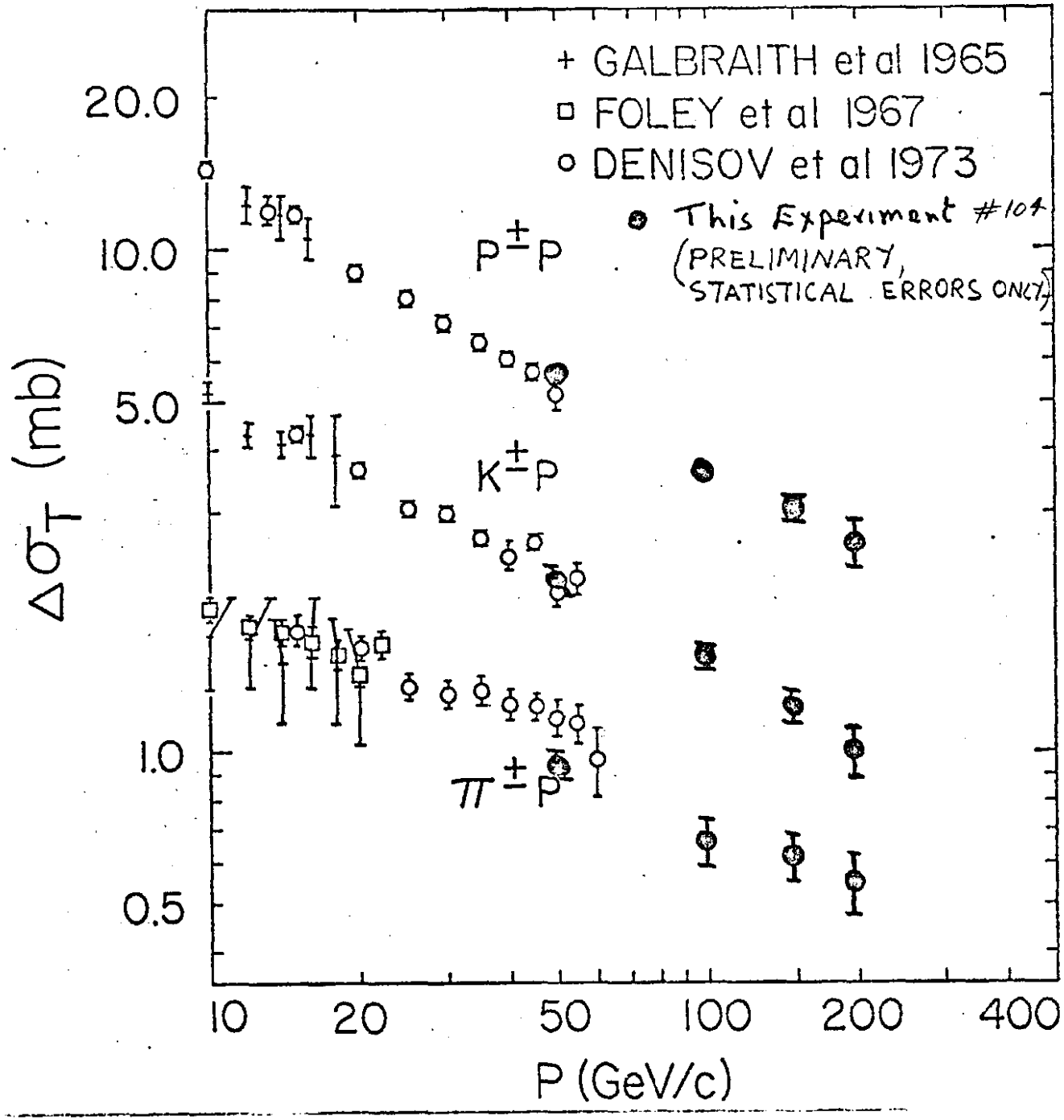
+ GALBRAITH et al 1965
□ FOLEY et al 1967
○ DENISOV et al 1973
● This Experiment #104
(PRELIMINARY, STATISTICAL ERRORS ONLY)
$P^{\pm}P$
$K^{\pm}P$
$\pi^{\pm}P$
$\Delta\sigma_T$ (mb)
20.0
10.0
5.0
1.0
0.5
10
20
50
100
200
400
P (GeV/c)

Fig. 16

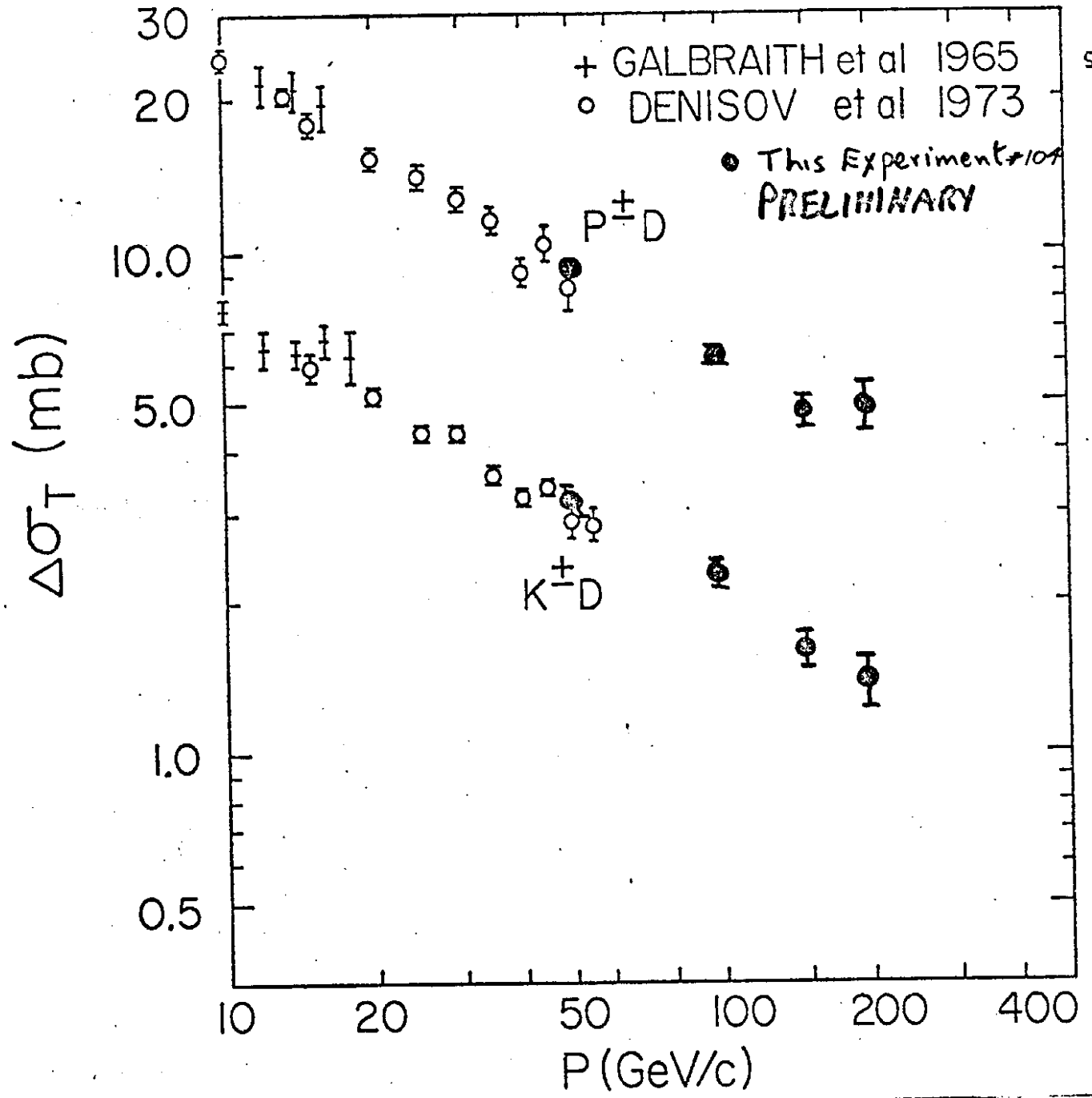
+ GALBRAITH et al 1965
o DENISOV et al 1973
• This Experiment
PRELIMINARY
5/6/74
$P^{\pm}D$
$K^{\pm}D$
$\Delta\sigma_T$ (mb)
P (GeV/c)
30
20
10.0
5.0
1.0
0.5
10
20
50
100
200
400

Fig. 17

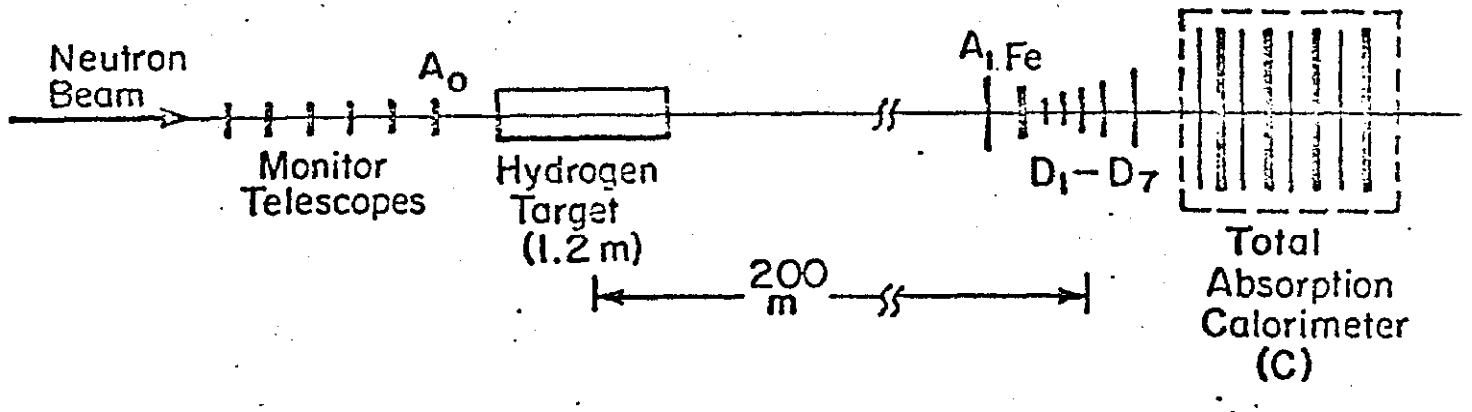
Neutron
Beam
A_o
Monitor
Telescopes
Hydrogen
Target
(1.2 m)
200
m
A_1 Fe
$D_1 - D_7$
Total
Absorption
Calorimeter
(C)

Fig. 18

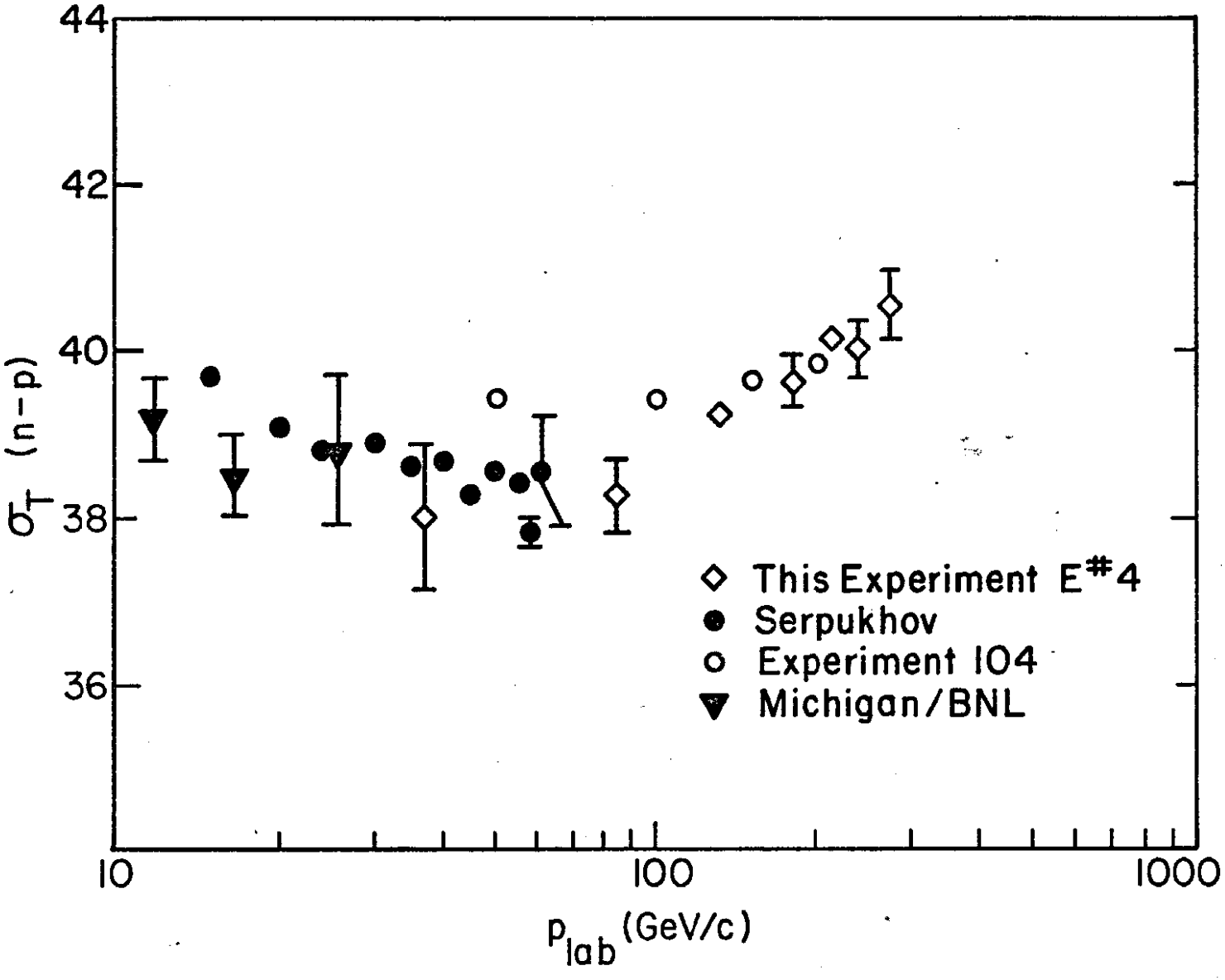
44
42
40
38
36
σ_T (n-p)
10
100
1000
p_{lab} (GeV/c)
This Experiment E#4
Serpukhov
Experiment 104
Michigan/BNL

Fig. 19

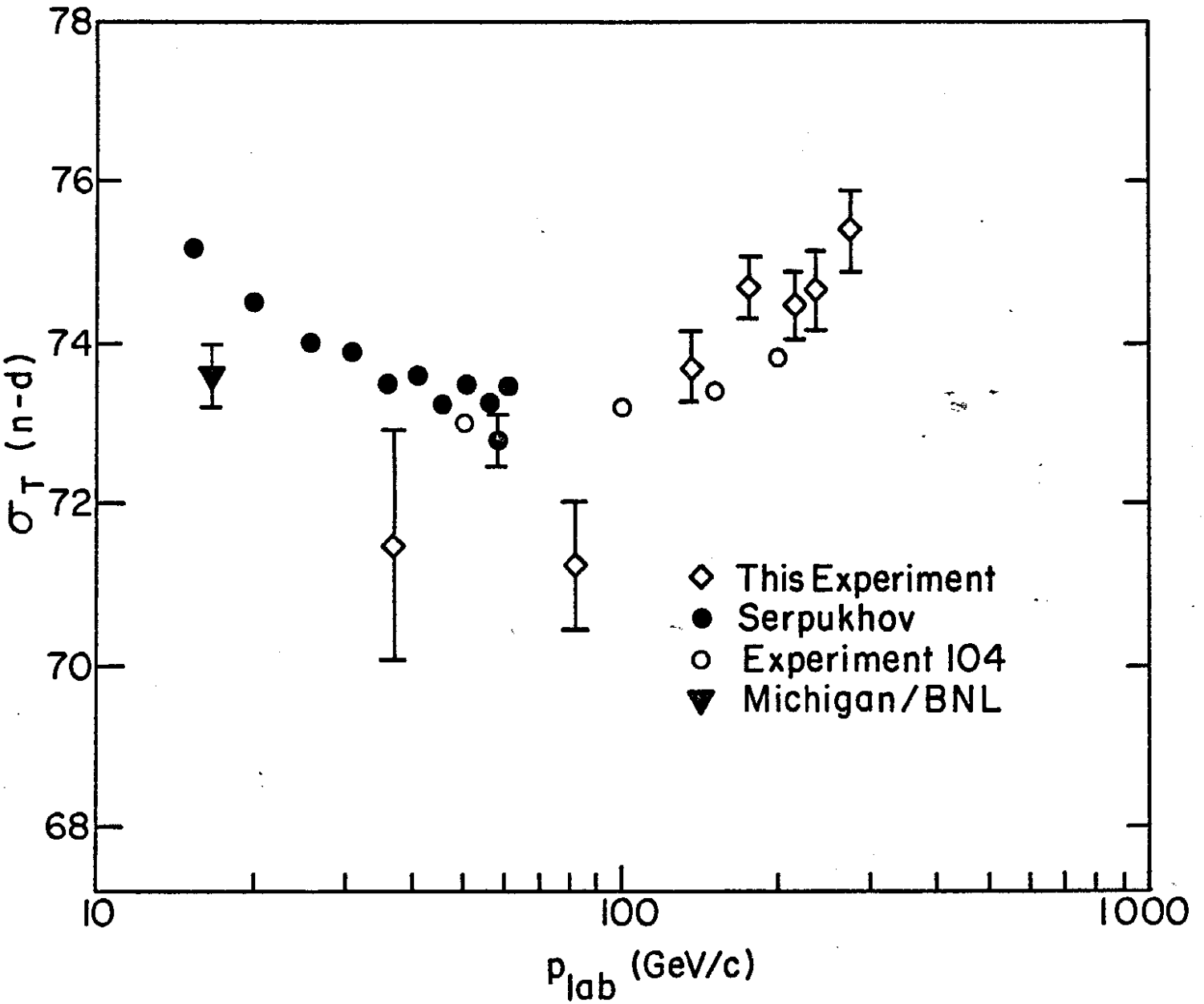
78
76
74
72
70
68
σ_T (n-d)
10
100
1000
p_{lab} (GeV/c)
This Experiment
Serpukhov
Experiment 104
Michigan/BNL

Fig. 20

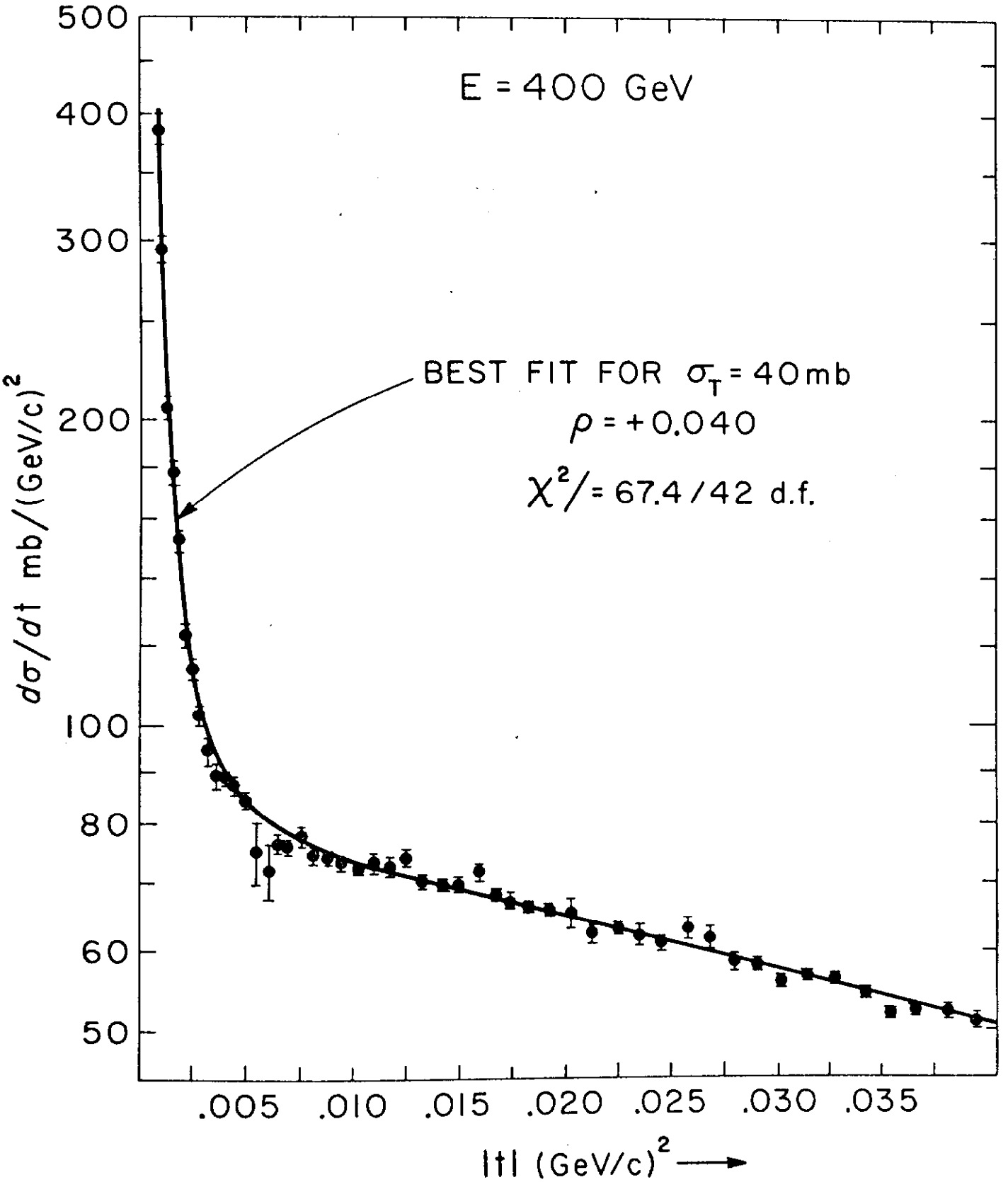
E = 400 GeV
BEST FIT FOR σ_T = 40mb
ρ = +0.040
χ^2/ = 67.4/42 d.f.
$d\sigma/dt$ mb/(GeV/c)^2
500
400
300
200
100
80
60
50
.005
.010
.015
.020
.025
.030
.035
|t| (GeV/c)^2 ⟶

Fig. 21

SINGLE ARM SPECTROMETER FACILITY

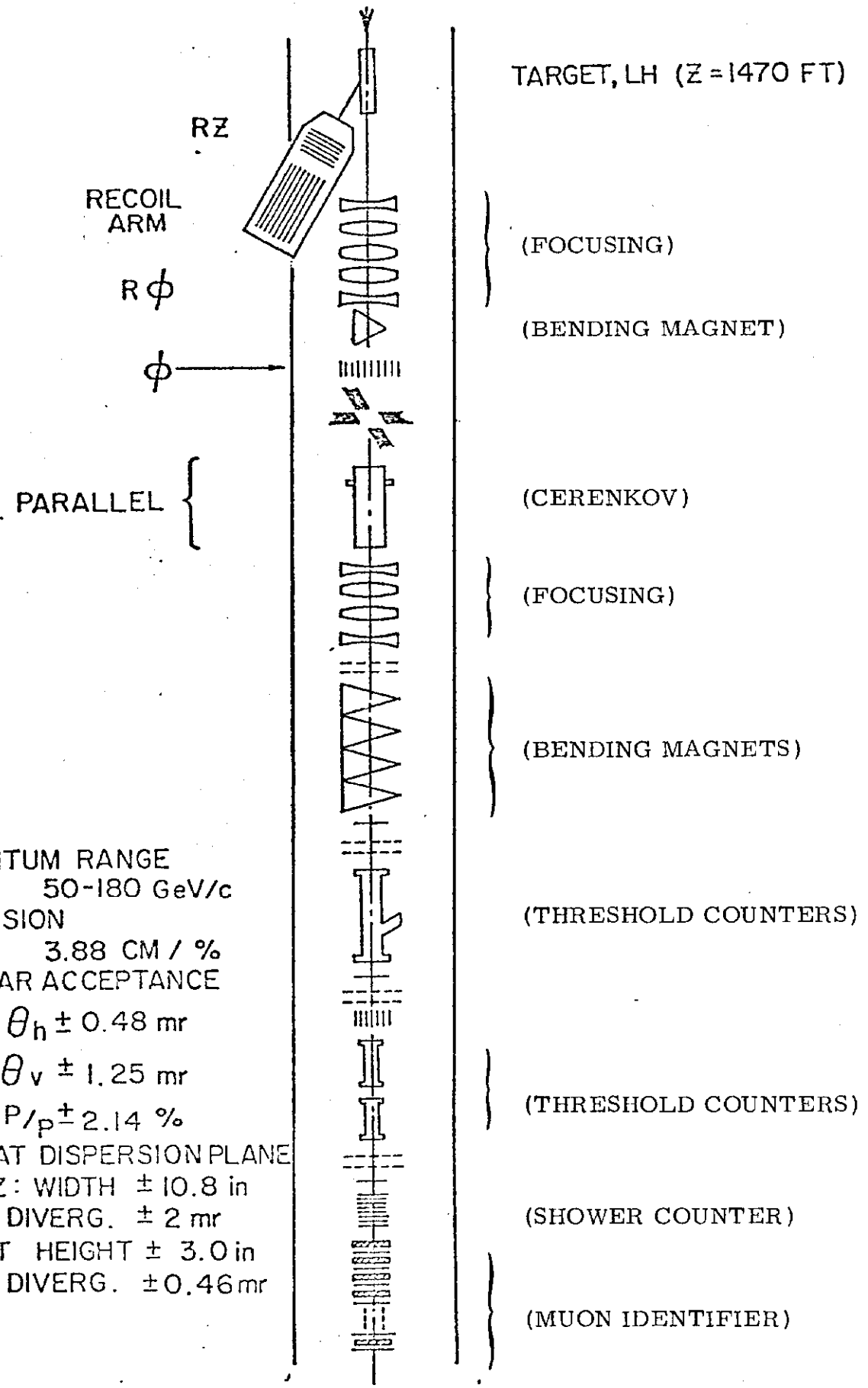

Fig. 22

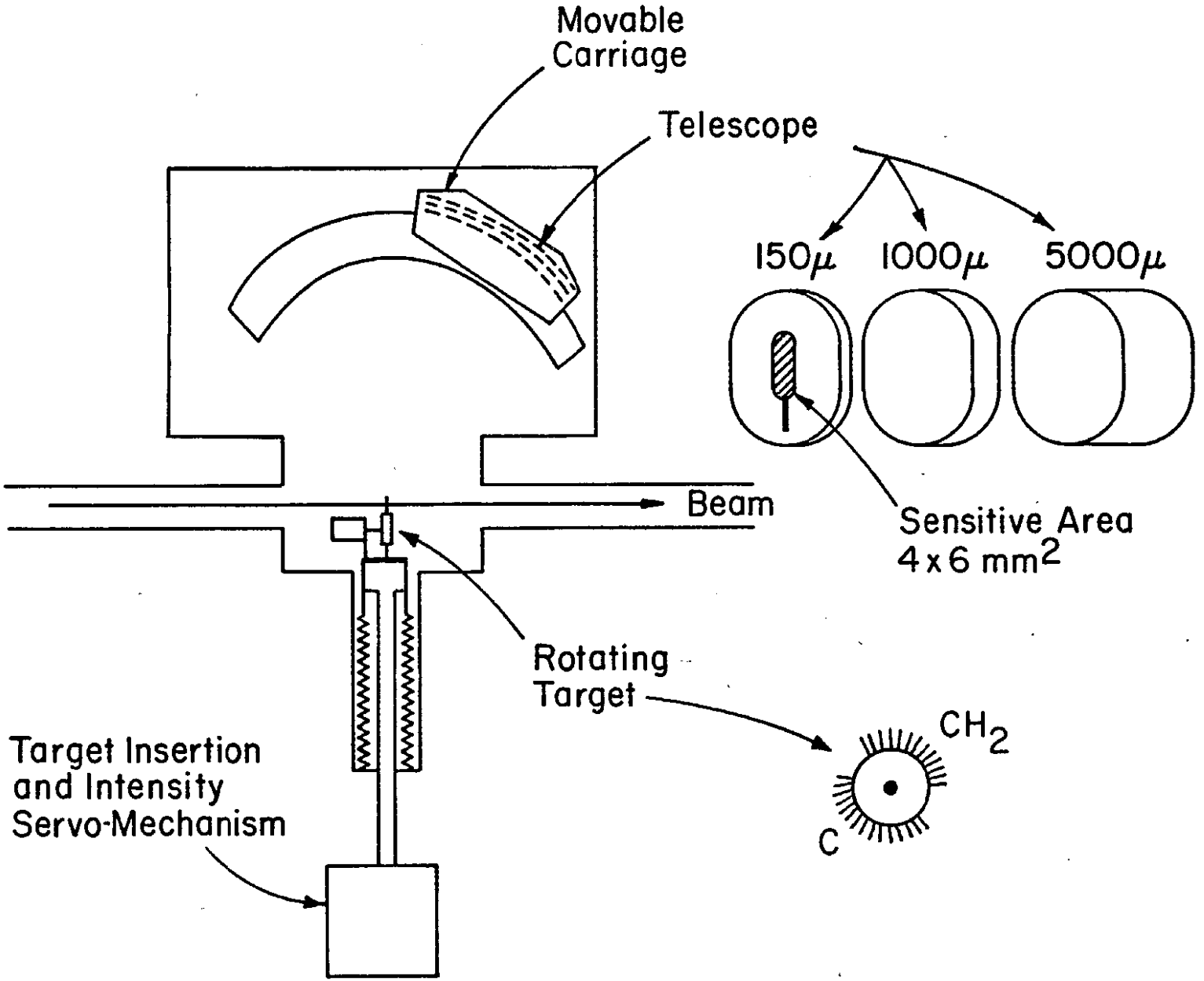
Movable
Carriage
Telescope
150μ
1000μ
5000μ
Beam
Sensitive Area
4x6 mm2
Rotating
Target
CH2
C
Target Insertion
and Intensity
Servo-Mechanism

Fig. 23

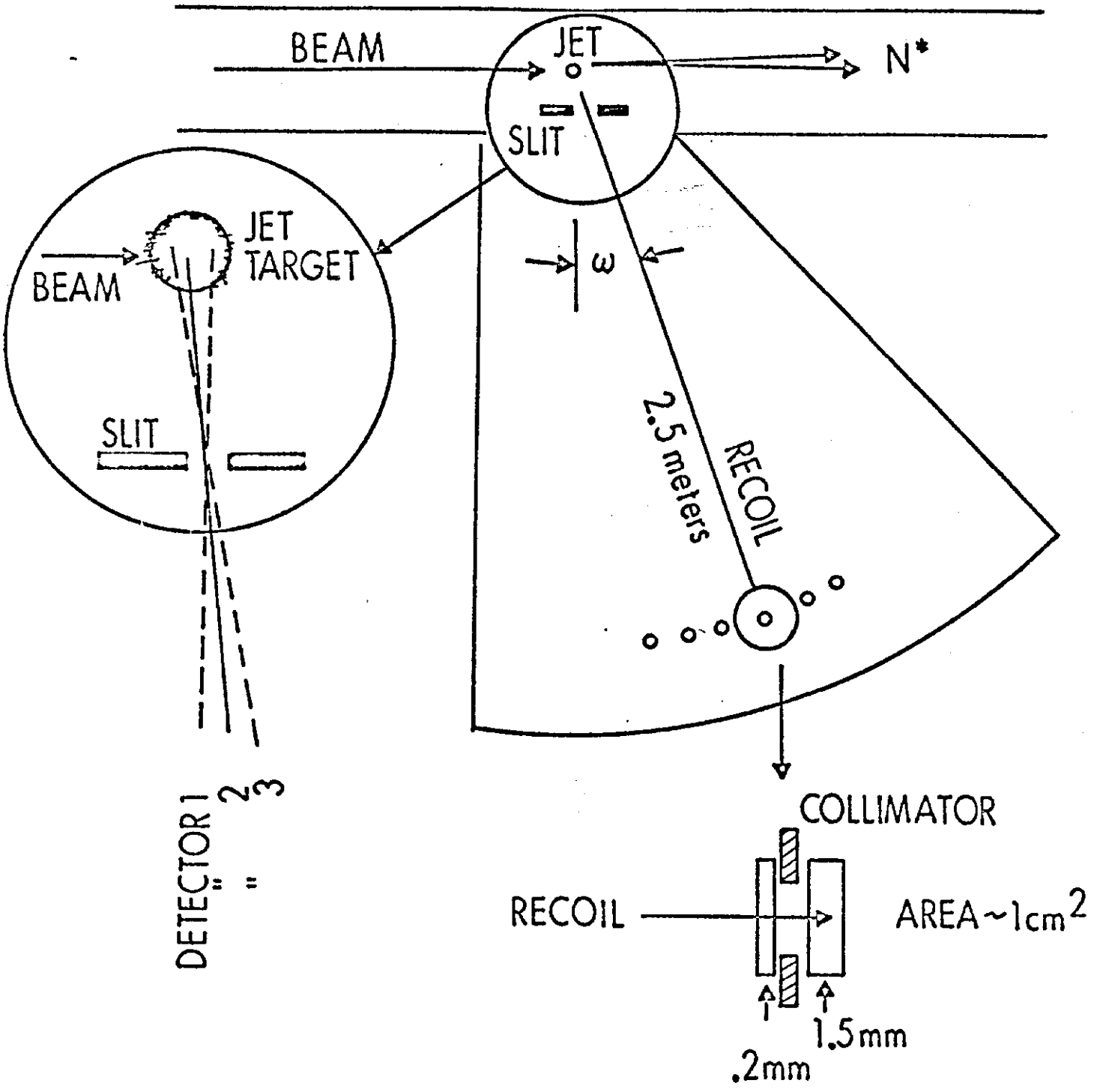
BEAM
JET
N*
SLIT
JET
TARGET
BEAM
SLIT
ω
2.5 meters
RECOIL
DETECTOR 1 2 3
COLLIMATOR
RECOIL
AREA ~ 1cm²
1.5mm
.2mm

Fig. 24

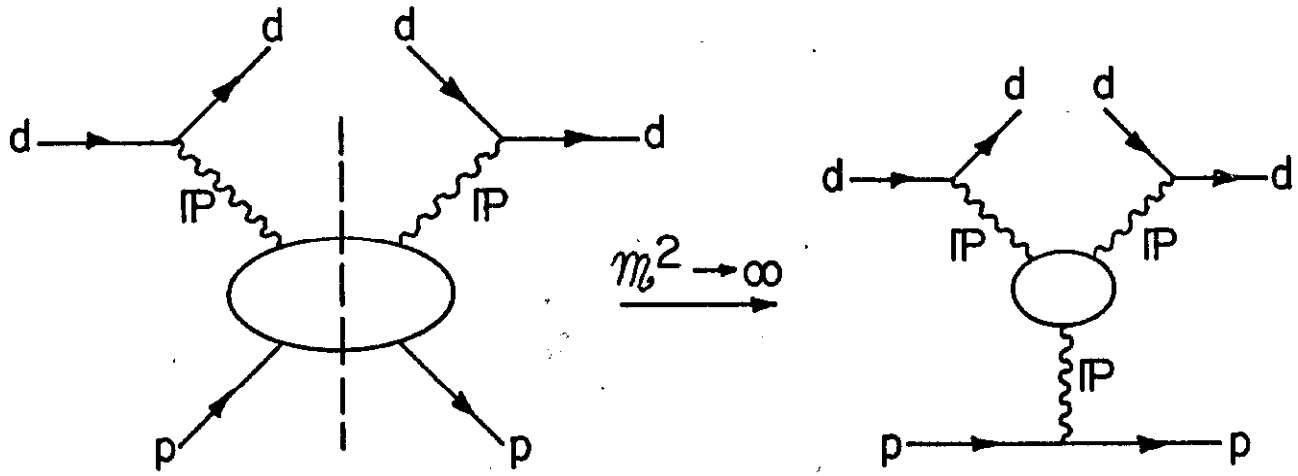

$$\int_0^N d\nu\, \nu \frac{d\sigma}{dt d\nu}(dp \to dX) = \frac{G^p_{pp}(t)\, N^{3-2\alpha_p(t)}}{3-2\alpha_p(t)}$$

Fig. 25

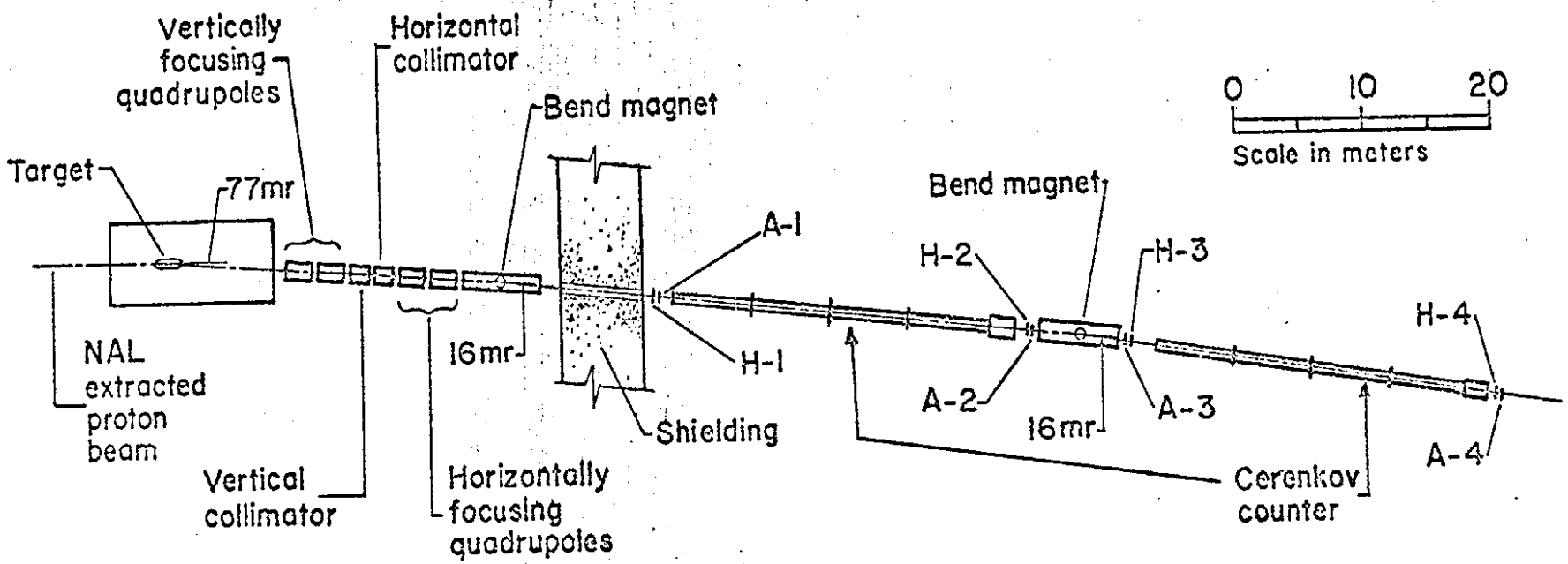
Vertically focusing quadrupoles
Horizontal collimator
Bend magnet
0 10 20
Scale in meters
Target
77mr
Bend magnet
A-1
H-2
H-3
H-4
NAL extracted proton beam
16mr
H-1
A-2
A-3
16mr
A-4
Shielding
Vertical collimator
Horizontally focusing quadrupoles
Cerenkov counter

Fig. 26

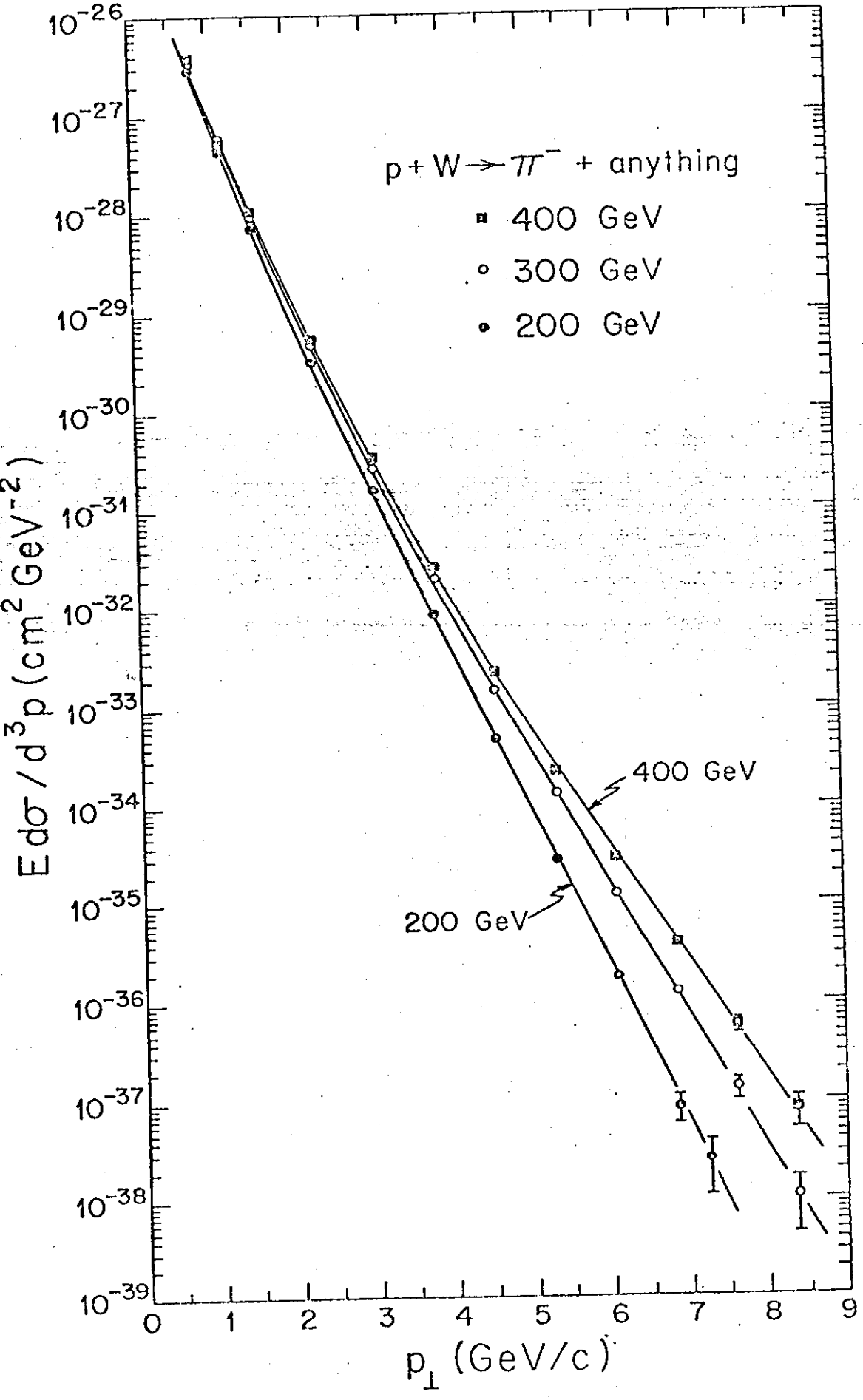
$p + W \rightarrow \pi^- +$ anything
400 GeV
300 GeV
200 GeV
400 GeV
200 GeV
$E d\sigma / d^3p$ (cm^2 GeV^{-2})
$p_\perp$ (GeV/c)
10^{-26}
10^{-27}
10^{-28}
10^{-29}
10^{-30}
10^{-31}
10^{-32}
10^{-33}
10^{-34}
10^{-35}
10^{-36}
10^{-37}
10^{-38}
10^{-39}
0 1 2 3 4 5 6 7 8 9

Fig. 27

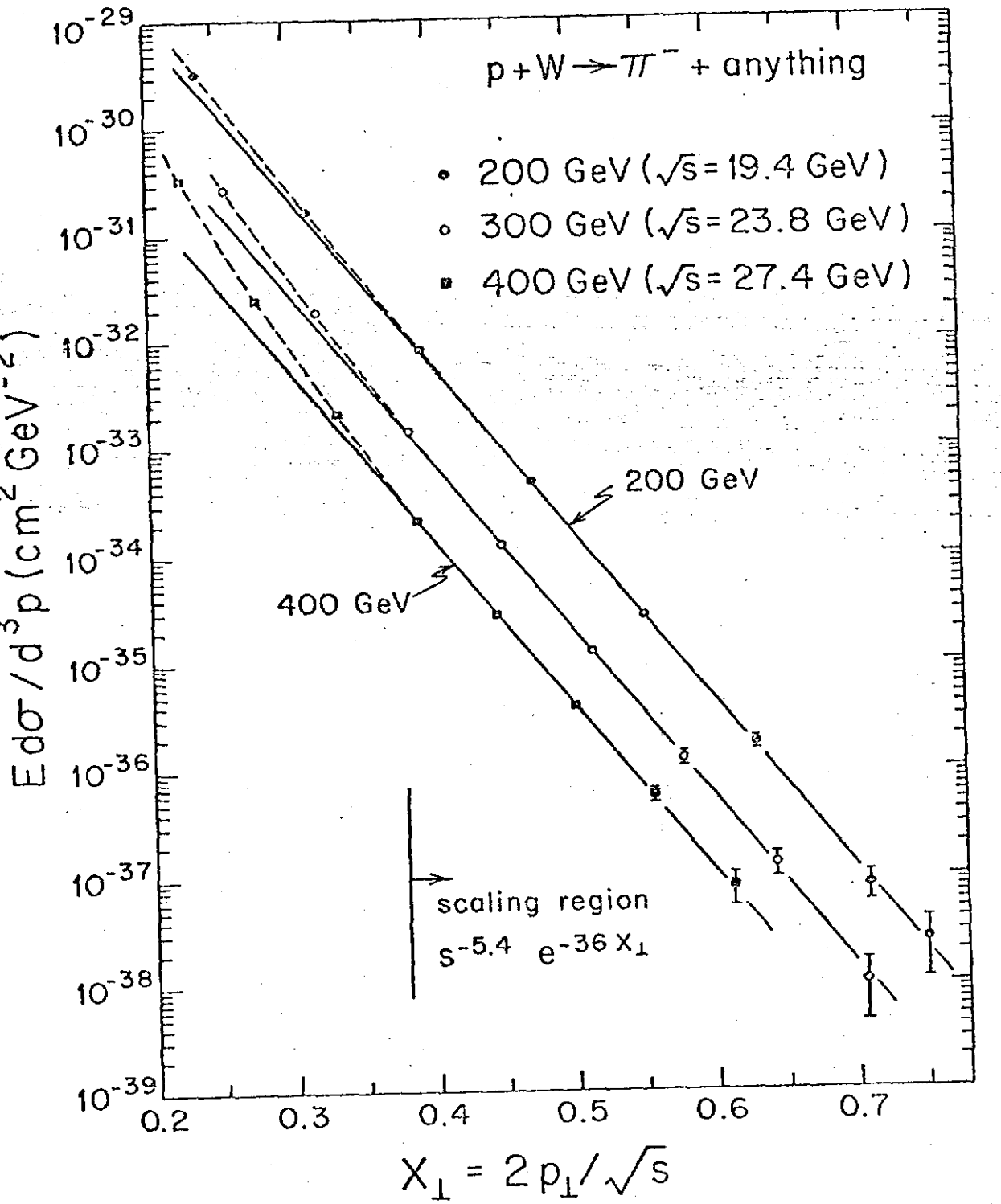
p + W → π⁻ + anything
200 GeV (√s = 19.4 GeV)
300 GeV (√s = 23.8 GeV)
400 GeV (√s = 27.4 GeV)
200 GeV
400 GeV
scaling region
s^-5.4 e^-36 X⊥
E dσ/d³p (cm² GeV⁻²)
X⊥ = 2p⊥/√s
10^-29
10^-30
10^-31
10^-32
10^-33
10^-34
10^-35
10^-36
10^-37
10^-38
10^-39
0.2
0.3
0.4
0.5
0.6
0.7

Fig. 28

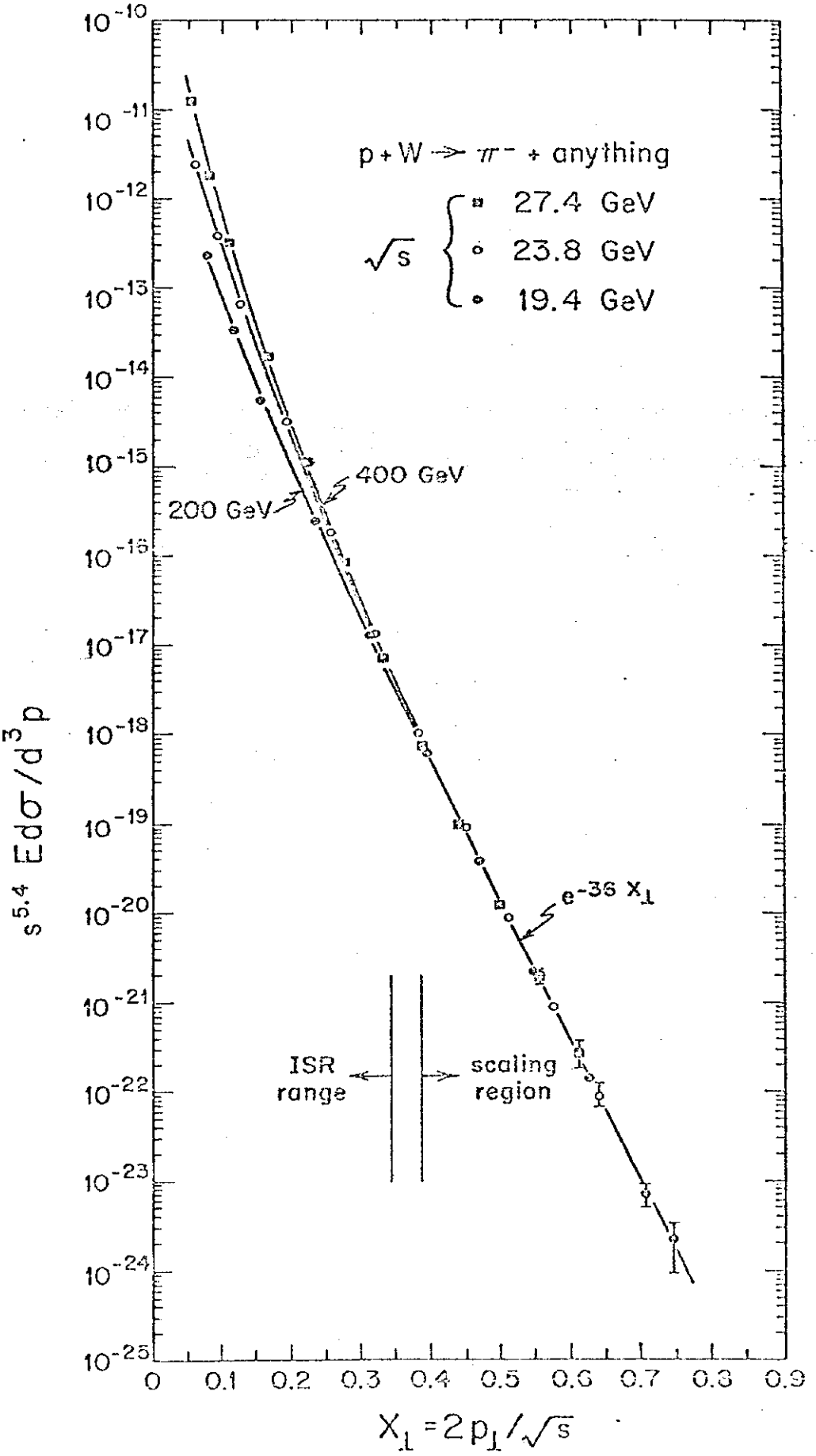
p + W → π⁻ + anything
√s
27.4 GeV
23.8 GeV
19.4 GeV
200 GeV
400 GeV
e-36 X⊥
ISR range
scaling region
s^5.4 Edσ/d³p
X⊥ = 2p⊥/√s
10^-10
10^-11
10^-12
10^-13
10^-14
10^-15
10^-16
10^-17
10^-18
10^-19
10^-20
10^-21
10^-22
10^-23
10^-24
10^-25
0
0.1
0.2
0.3
0.4
0.5
0.6
0.7
0.8
0.9

Fig. 29

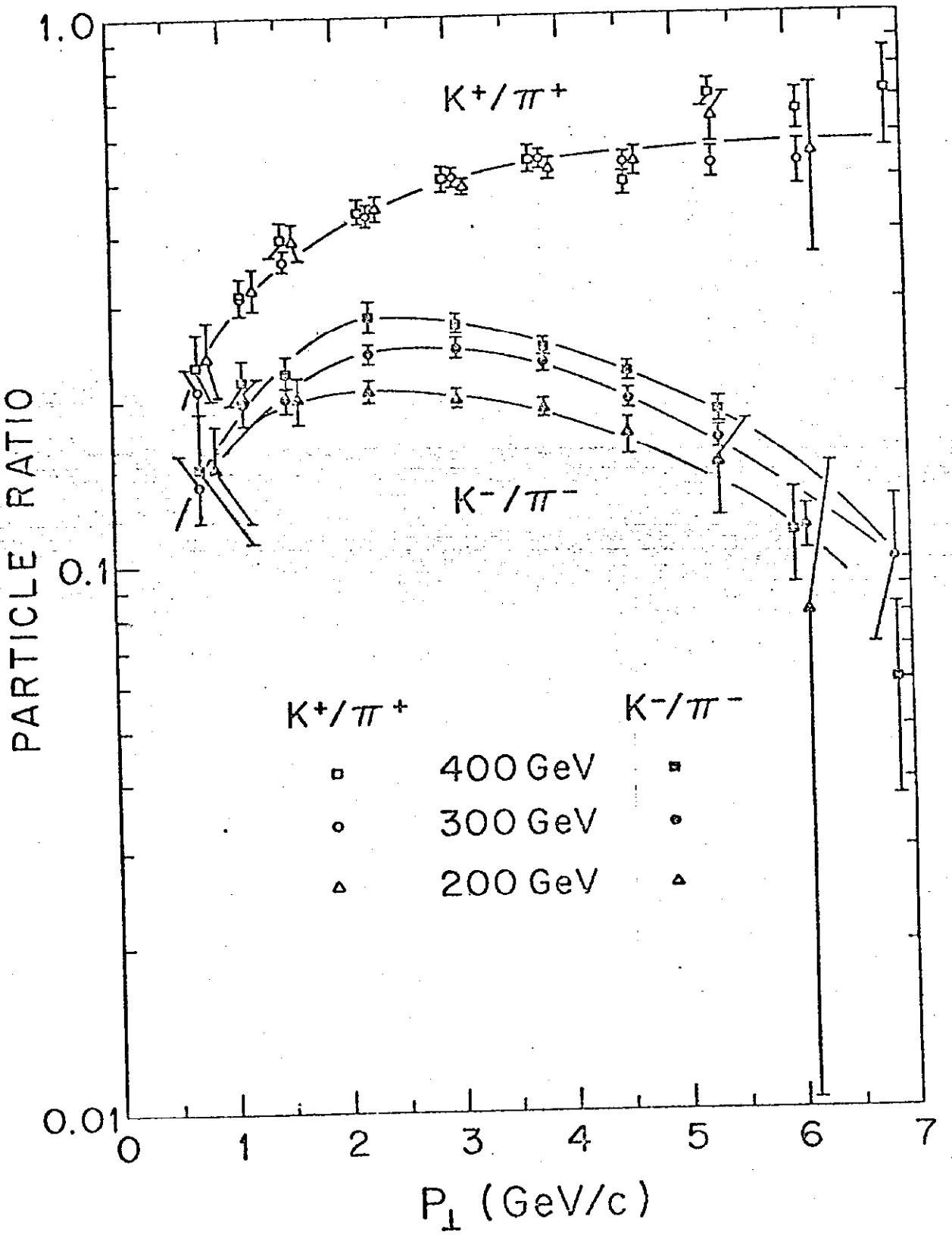
1.0
0.1
0.01
PARTICLE RATIO
K+/π+
K-/π-
K+/π+
K-/π-
400 GeV
300 GeV
200 GeV
0
1
2
3
4
5
6
7
P⊥ (GeV/c)

Fig. 30

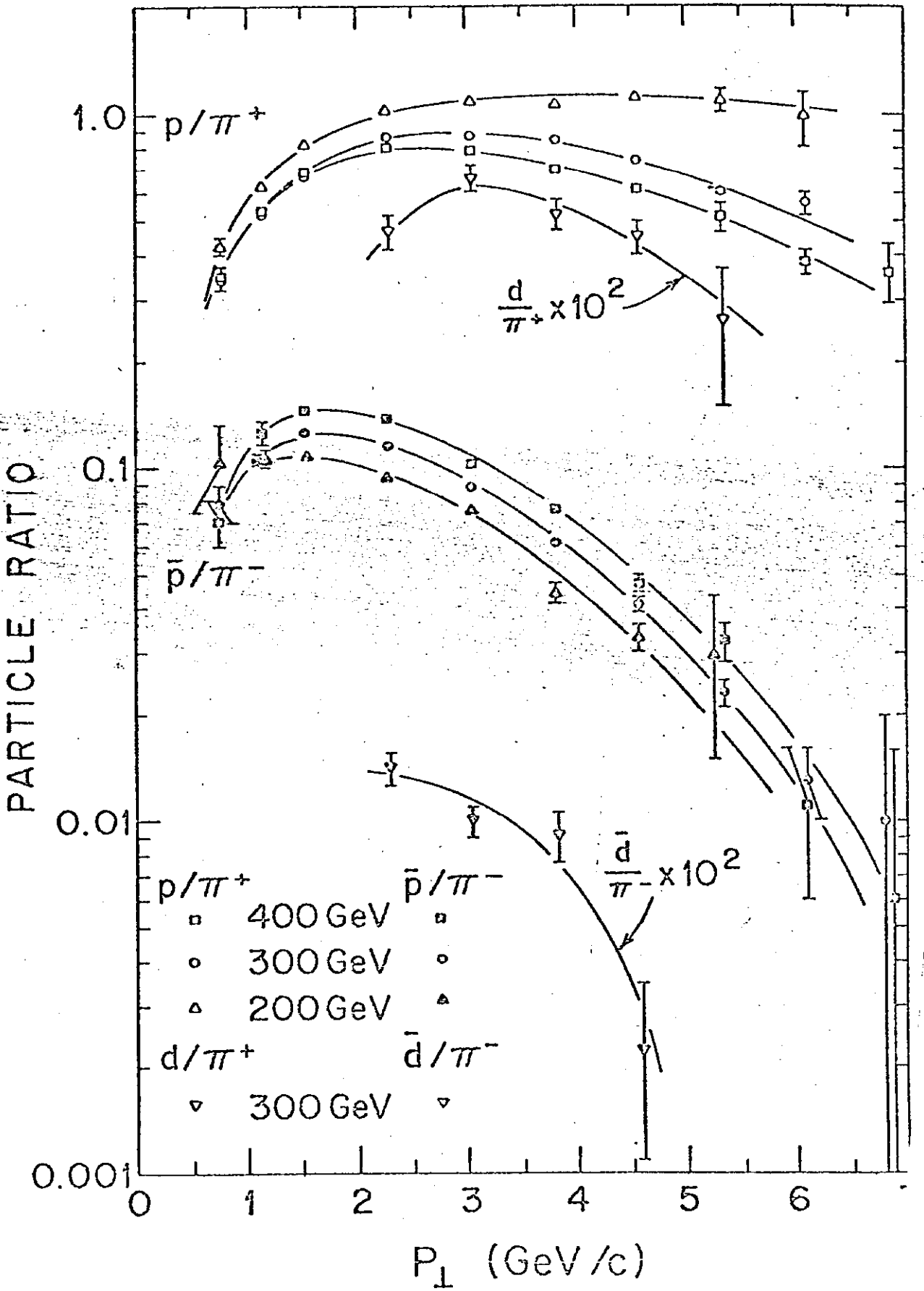
1.0
0.1
0.01
0.001
PARTICLE RATIO
p/π+
d/π+ x10^2
p̄/π−
d̄/π− x10^2
p/π+
400 GeV
300 GeV
200 GeV
d/π+
300 GeV
p̄/π−
d̄/π−
0
1
2
3
4
5
6
P⊥ (GeV/c)

Fig. 31

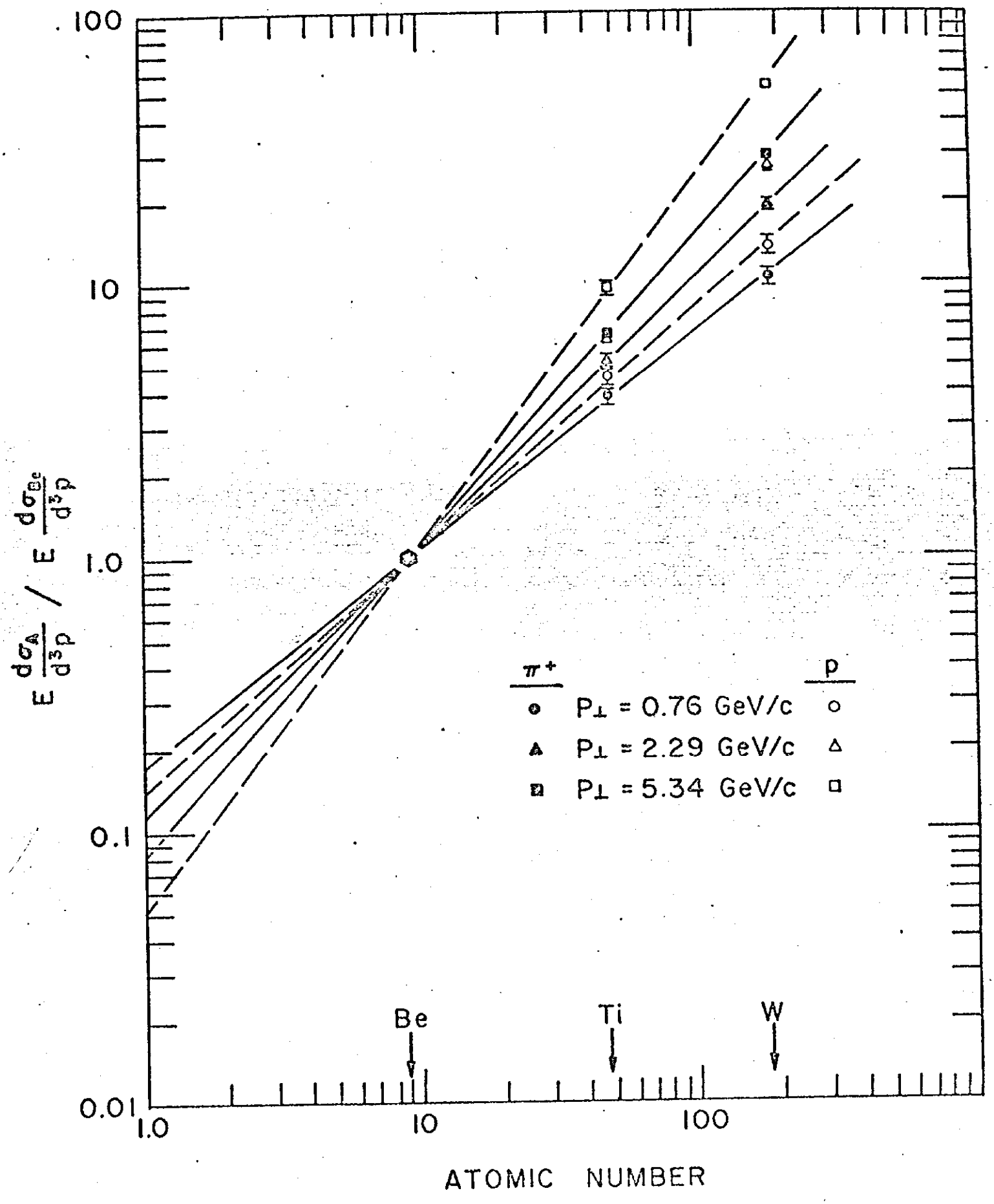
100
10
1.0
0.1
0.01
1.0
10
100
$E\frac{d\sigma_A}{d^3p} / E\frac{d\sigma_{Be}}{d^3p}$
ATOMIC NUMBER
Be
Ti
W
π^+
p
$P_\perp$ = 0.76 GeV/c
$P_\perp$ = 2.29 GeV/c
$P_\perp$ = 5.34 GeV/c

Fig. 32

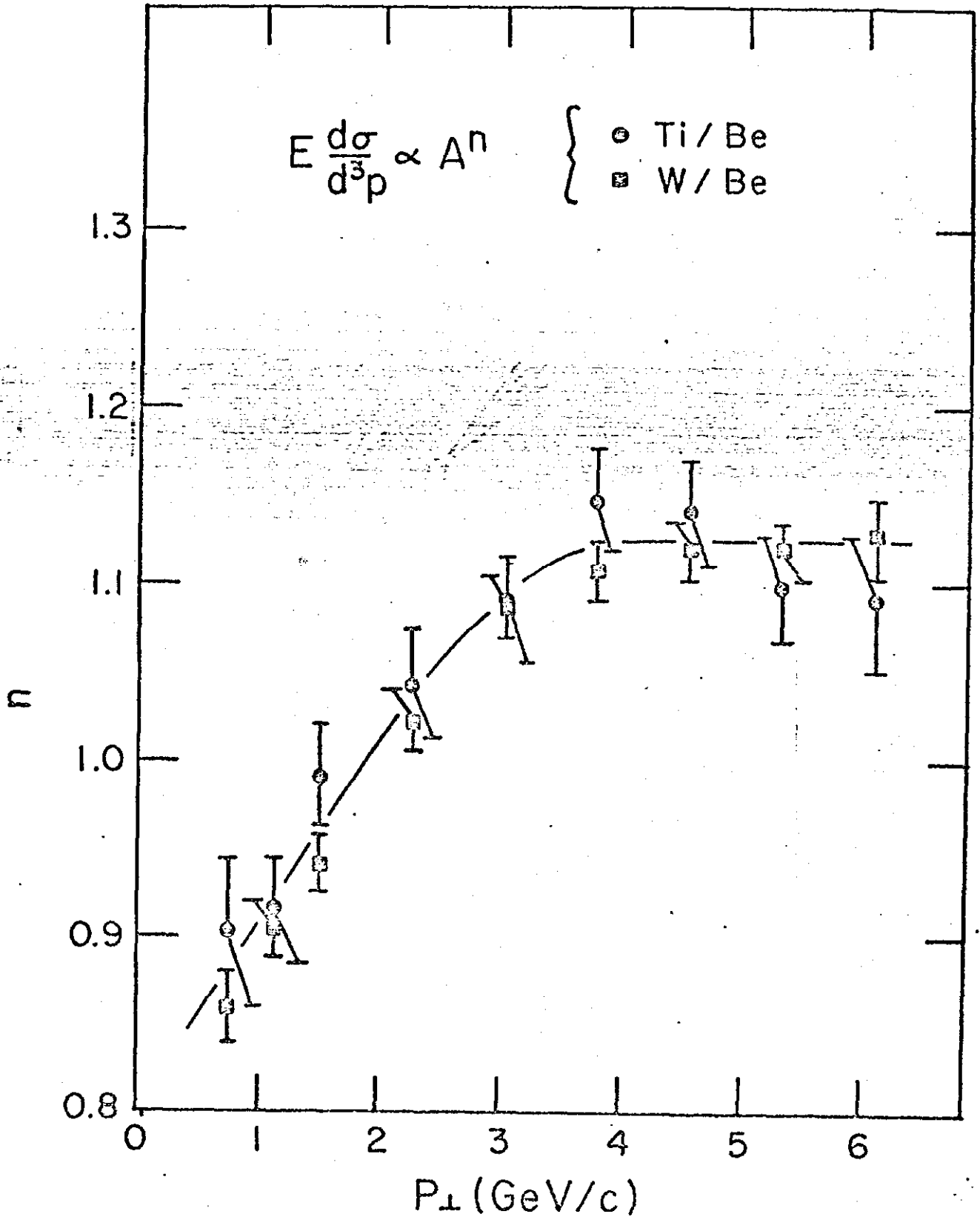
$E\frac{d\sigma}{d^3p} \propto A^n$
Ti / Be
W / Be
1.3
1.2
1.1
1.0
0.9
0.8
n
0
1
2
3
4
5
6
$P_\perp$ (GeV/c)

Fig. 33

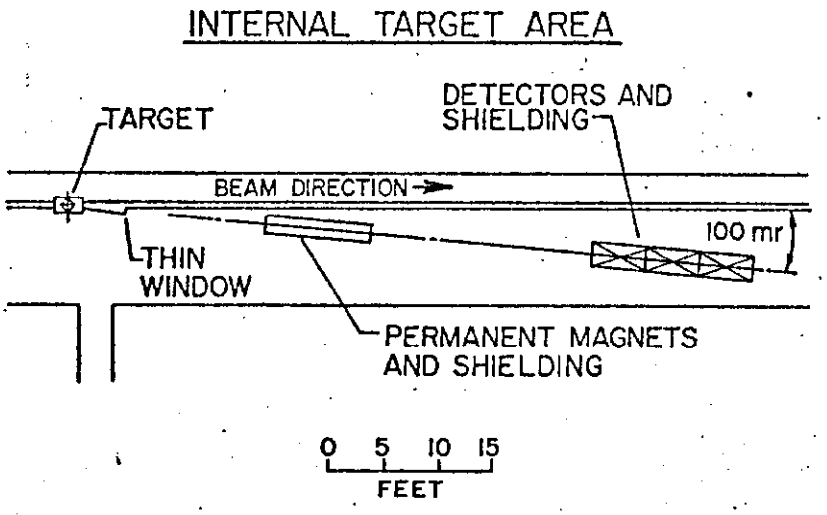
INTERNAL TARGET AREA
TARGET
DETECTORS AND SHIELDING
BEAM DIRECTION
100 mr
THIN WINDOW
PERMANENT MAGNETS AND SHIELDING
0 5 10 15
FEET

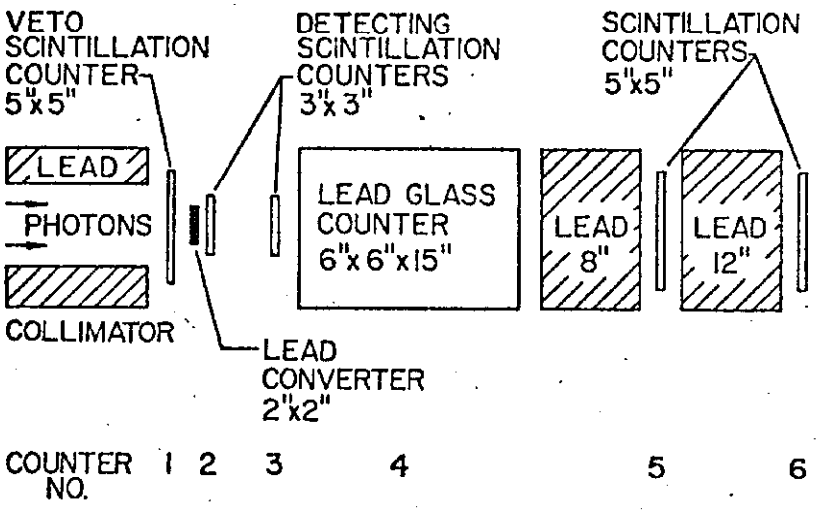
DETECTOR SYSTEM
VETO SCINTILLATION COUNTER 5"x5"
DETECTING SCINTILLATION COUNTERS 3"x3"
SCINTILLATION COUNTERS 5"x5"
LEAD
PHOTONS
COLLIMATOR
LEAD GLASS COUNTER 6"x6"x15"
LEAD 8"
LEAD 12"
LEAD CONVERTER 2"x2"
COUNTER NO. 1 2 3 4 5 6

Fig. 1

Fig. 34

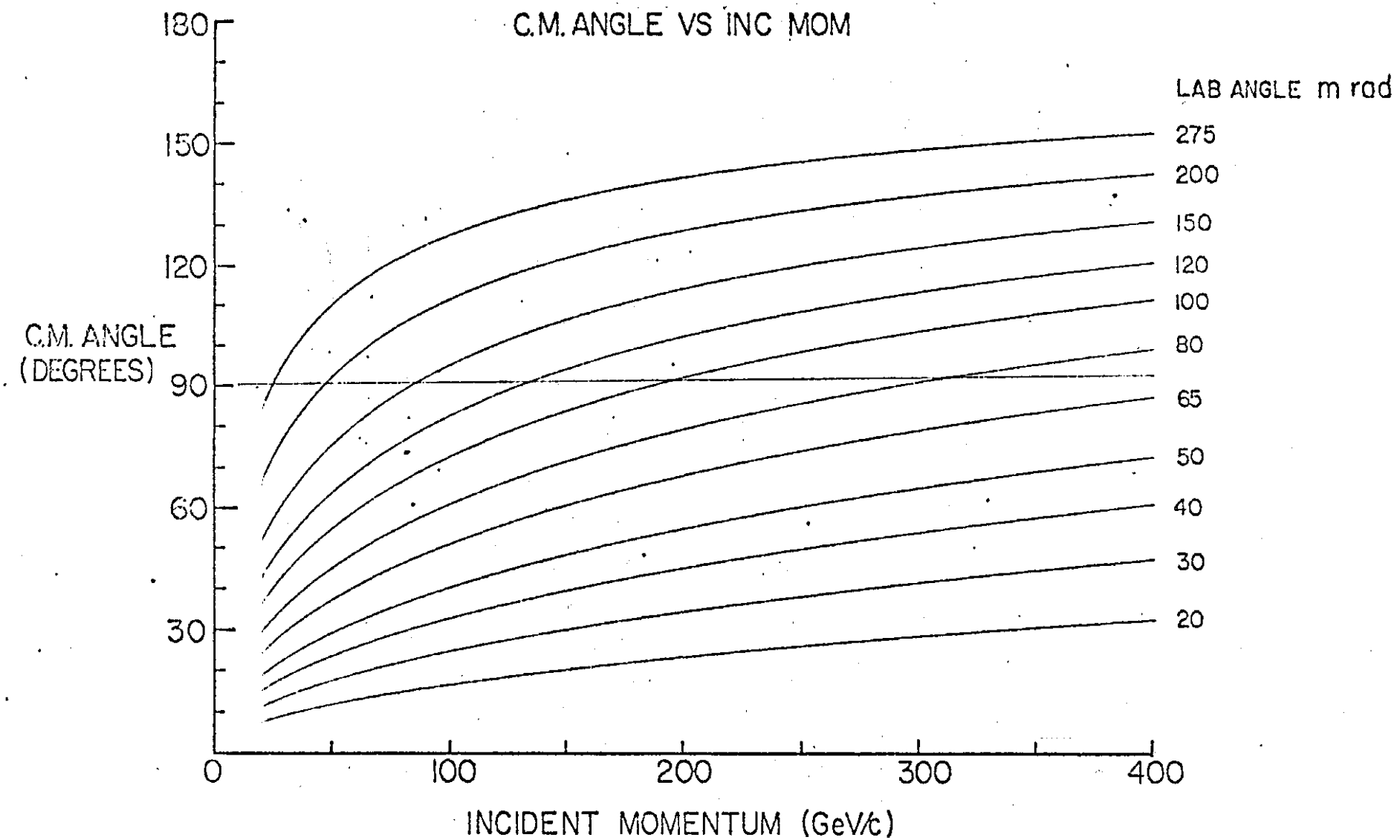
C.M. ANGLE VS INC MOM
LAB ANGLE m rad
275
200
150
120
100
80
65
50
40
30
20
C.M. ANGLE (DEGREES)
180
150
120
90
60
30
0
100
200
300
400
INCIDENT MOMENTUM (GeV/c)

Fig. 35

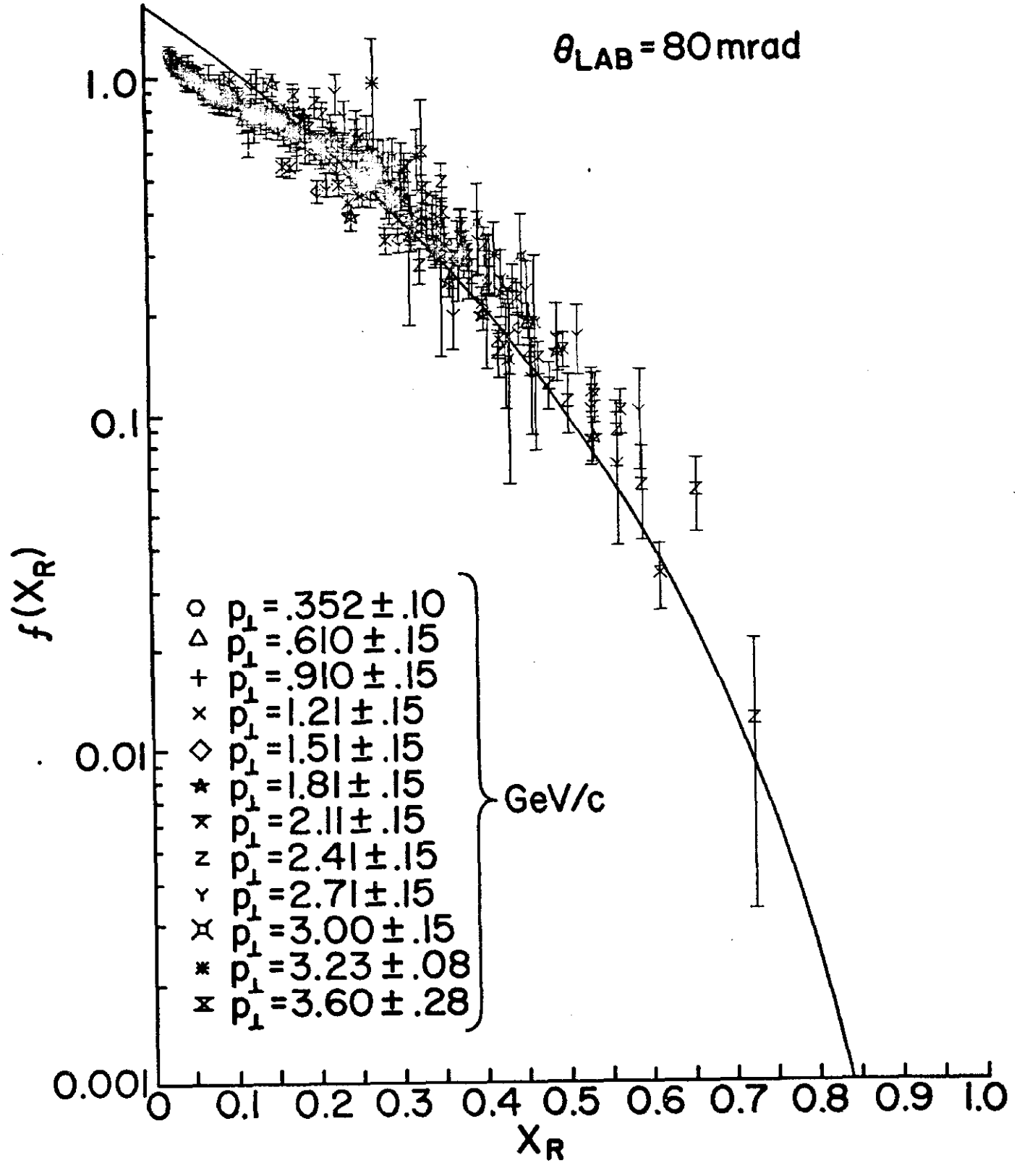
θ_{LAB} = 80 mrad
1.0
0.1
0.01
0.001
$f(X_R)$
$p_\perp$ = .352 ± .10
$p_\perp$ = .610 ± .15
$p_\perp$ = .910 ± .15
$p_\perp$ = 1.21 ± .15
$p_\perp$ = 1.51 ± .15
$p_\perp$ = 1.81 ± .15
$p_\perp$ = 2.11 ± .15
$p_\perp$ = 2.41 ± .15
$p_\perp$ = 2.71 ± .15
$p_\perp$ = 3.00 ± .15
$p_\perp$ = 3.23 ± .08
$p_\perp$ = 3.60 ± .28
GeV/c
0 0.1 0.2 0.3 0.4 0.5 0.6 0.7 0.8 0.9 1.0
X_R

Fig. 36

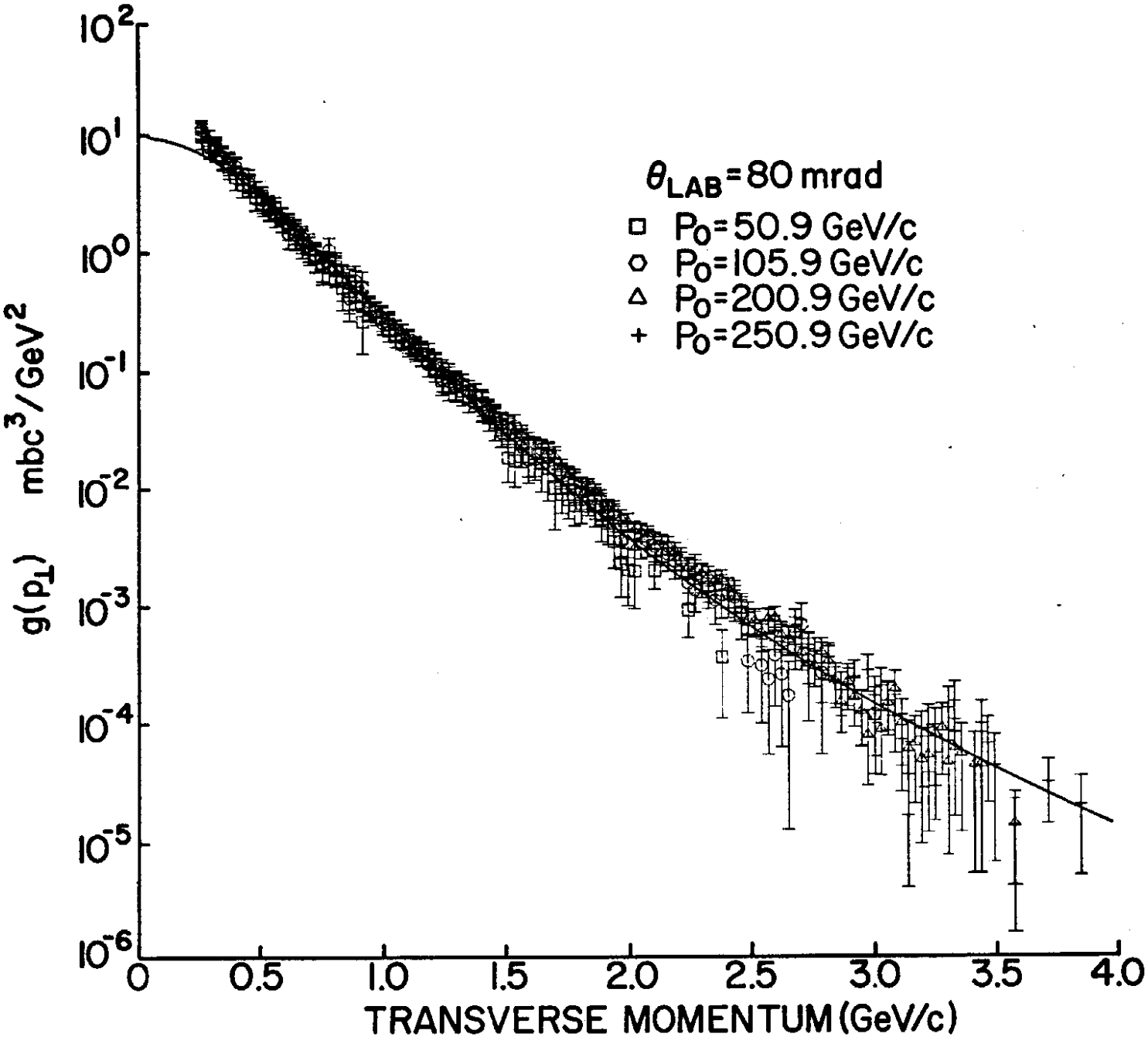
θ_{LAB}=80 mrad
P_0=50.9 GeV/c
P_0=105.9 GeV/c
P_0=200.9 GeV/c
P_0=250.9 GeV/c
$g(p_T)$ mbc^3/GeV^2
TRANSVERSE MOMENTUM (GeV/c)
10^2
10^1
10^0
10^{-1}
10^{-2}
10^{-3}
10^{-4}
10^{-5}
10^{-6}
0
0.5
1.0
1.5
2.0
2.5
3.0
3.5
4.0

Fig. 37

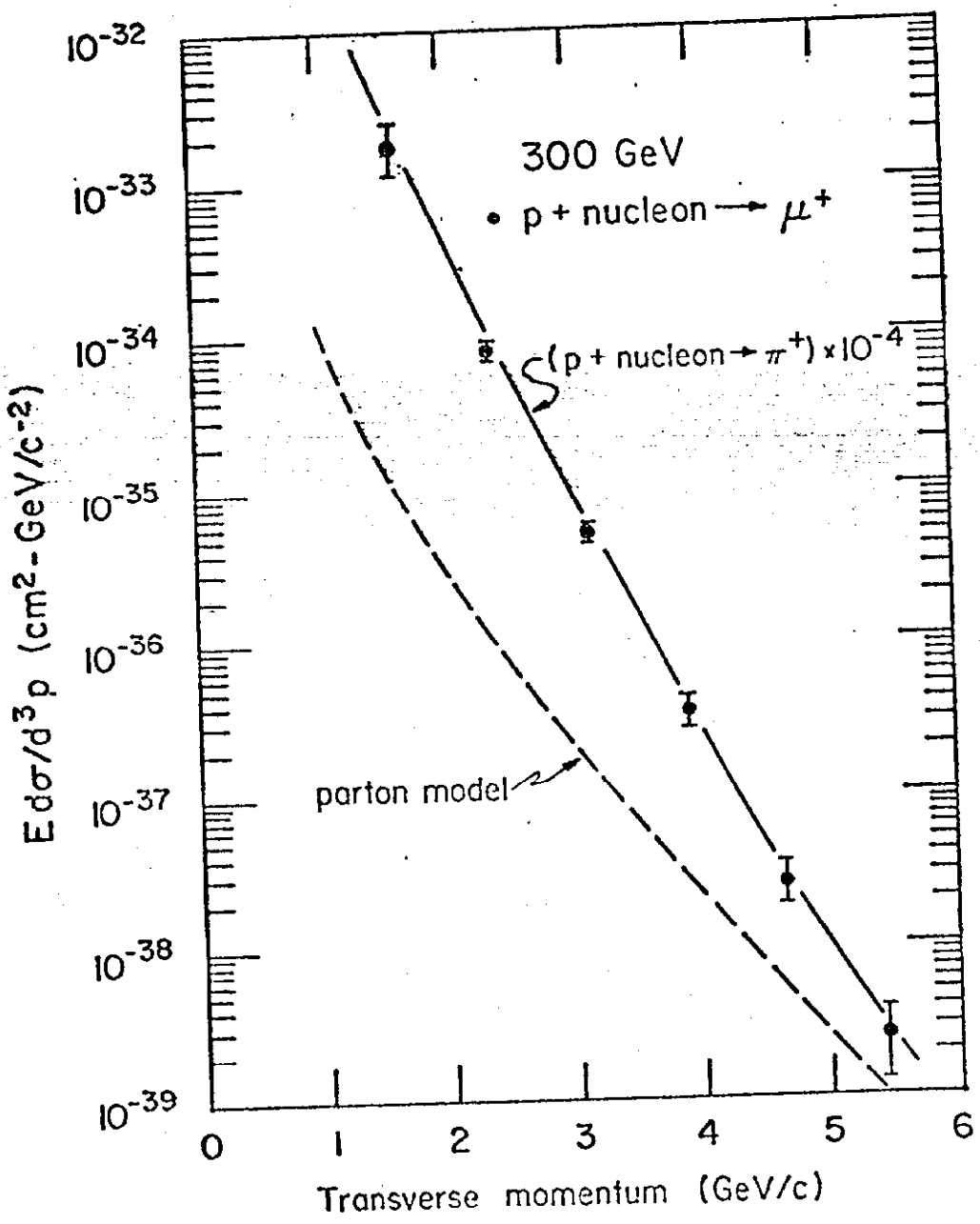
300 GeV
p + nucleon → μ+
(p + nucleon → π+) × 10-4
parton model
Ed σ/d3p (cm2 - GeV/c-2)
Transverse momentum (GeV/c)
10-32
10-33
10-34
10-35
10-36
10-37
10-38
10-39
0
1
2
3
4
5
6

Fig. 38

SCHEMATIC DIAGRAM OF LEPTON 70 APPARATUS
(ABRIDGED)

PURPOSE: To Measure Spectrum of High P_T Directly Produced Electrons

$$P_T = p \sin \Theta_H$$

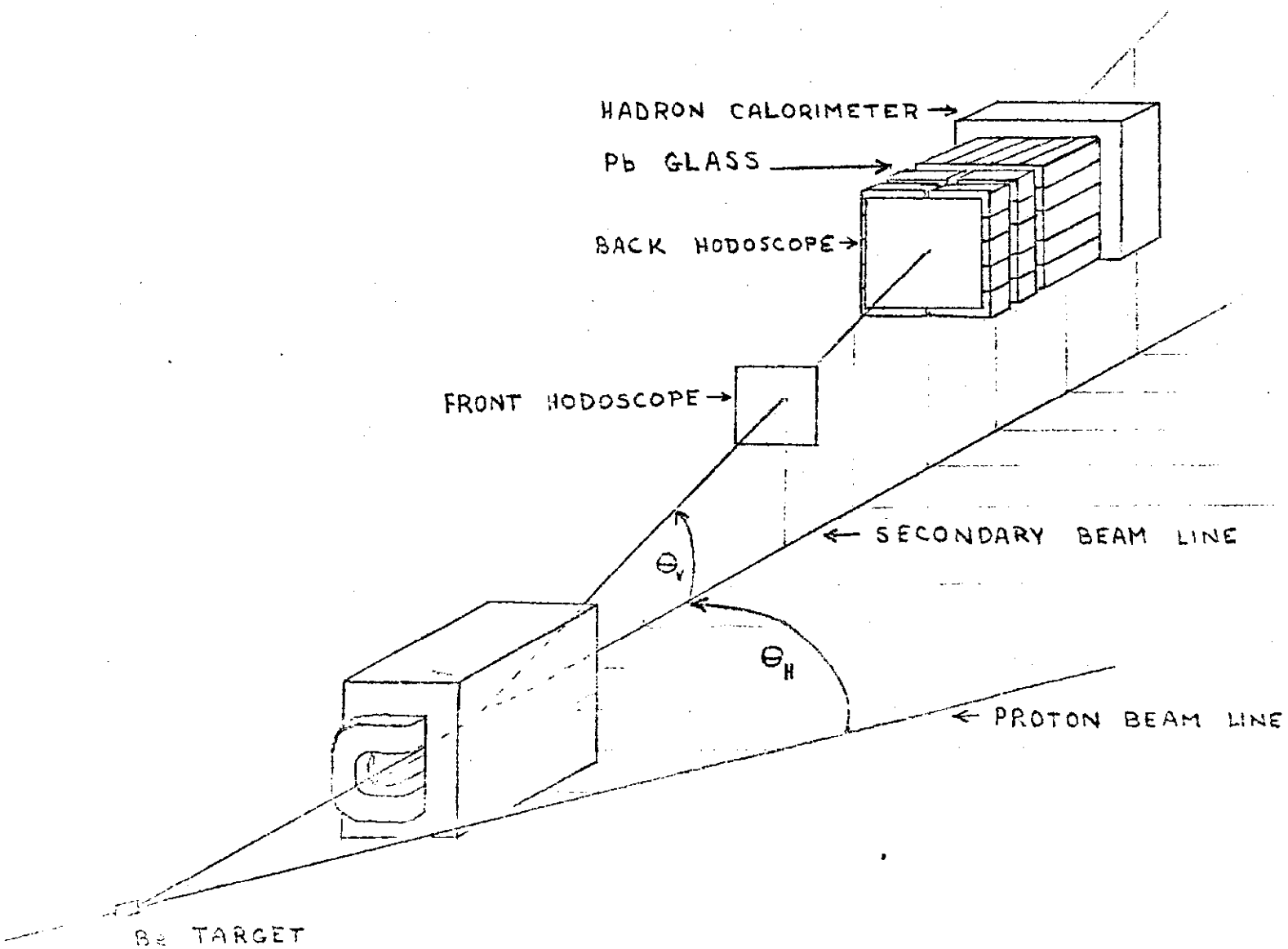

Fig. 39

DIRECT MUON PRODUCTION

. No. 184 (Chicago, Harvard, Pennsylvania, and Wisconsin), A1, A2, A3 - Hadron absorbers

8 GeV < E_p < 300 GeV Spectrometer magnet - B3 PC1-4: MWPC
S1-S8 counters

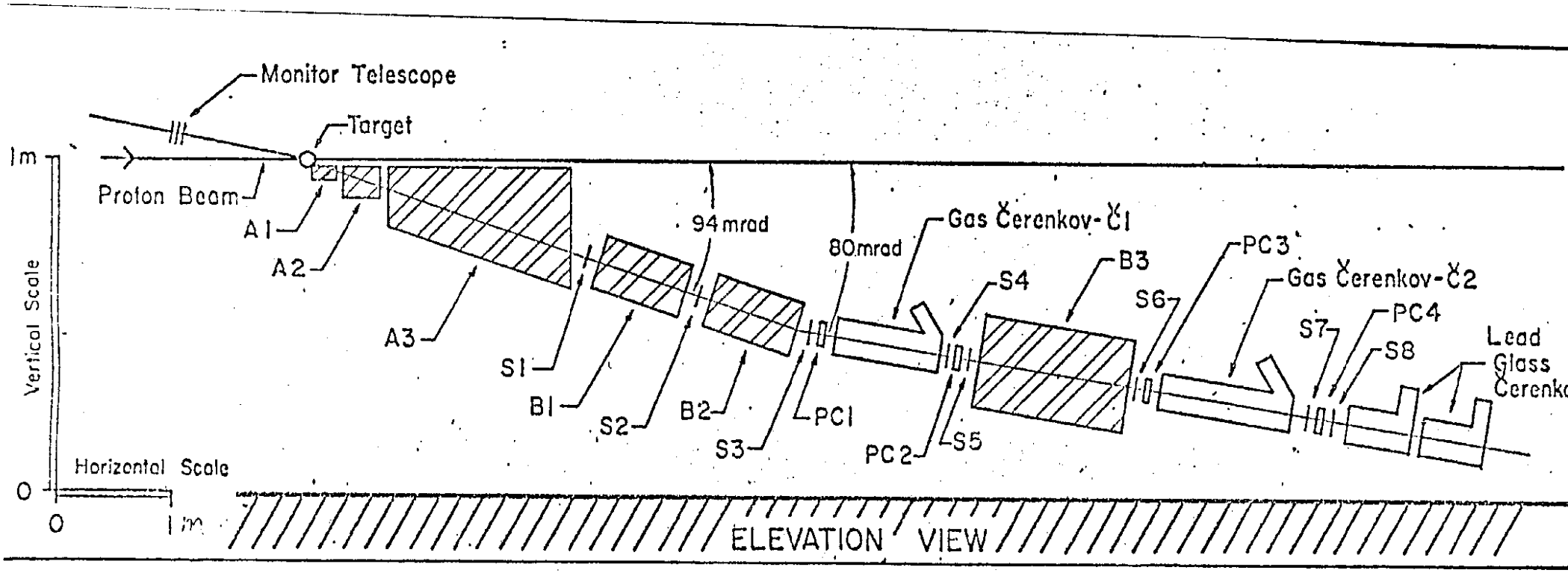

Fig. 40